



**16th International Conference
on Ion Sources**
August 23-28, 2015
New York City



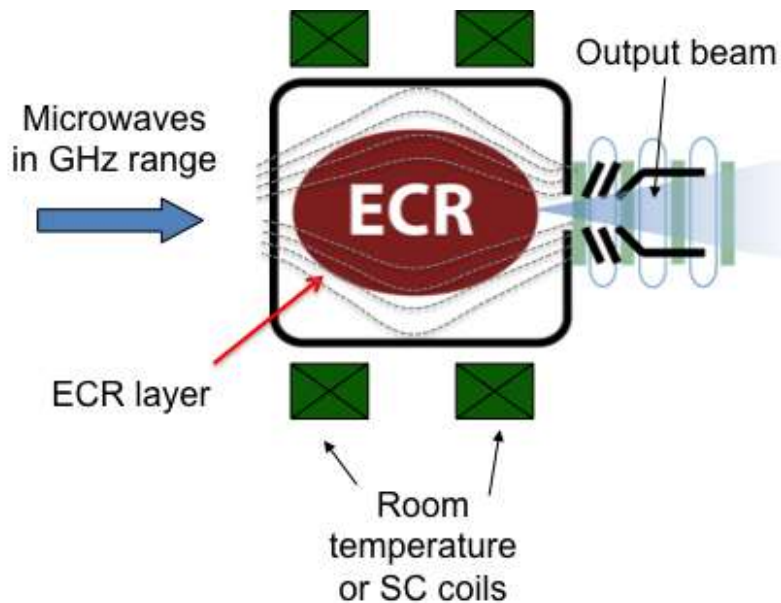
High density plasmas and new diagnostics

L. Celona, S. Gammino, D. Mascali

*Istituto Nazionale di Fisica Nucleare – Laboratori Nazionali del Sud
Via S. Sofia 62, 95123 Catania, ITALY*



Overcoming the actual limit of ECRIS



Plasma density, plasma temperature and ion confining times are the crucial parameters for establishing high ECRIS performances

ECRIS STD MODEL

$$n_e \propto \omega_{RF}^2$$

INTRINSIC
Density
limitation

1. **High Frequency Generators to increase the plasma density;**
2. **High Magnetic Fields to make longer the ions confining time;**

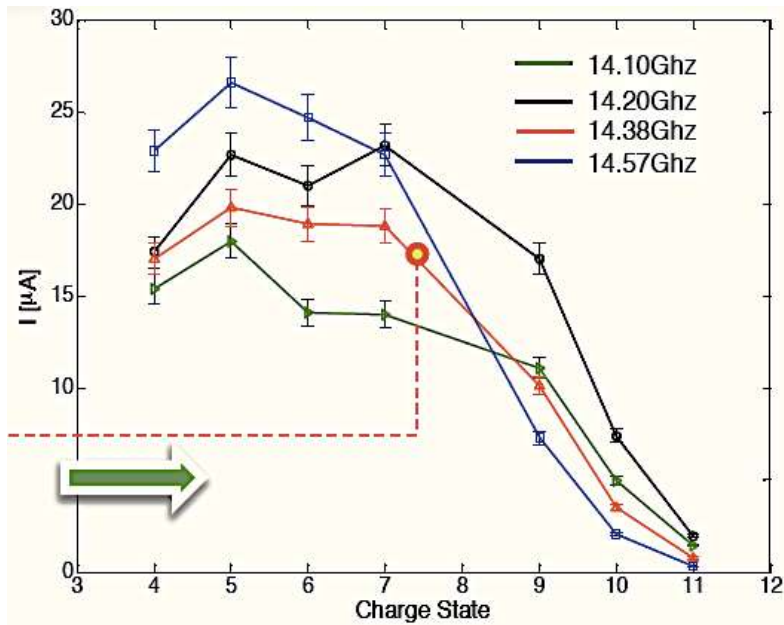
Brute force cannot be anymore used because of technological reasons (magnets, hot electrons generations, plasma overheating, cooling, ...)

Alternative heating schemes

Development of advanced diagnostics tools to make a step forward in understanding heating and confinement mechanism

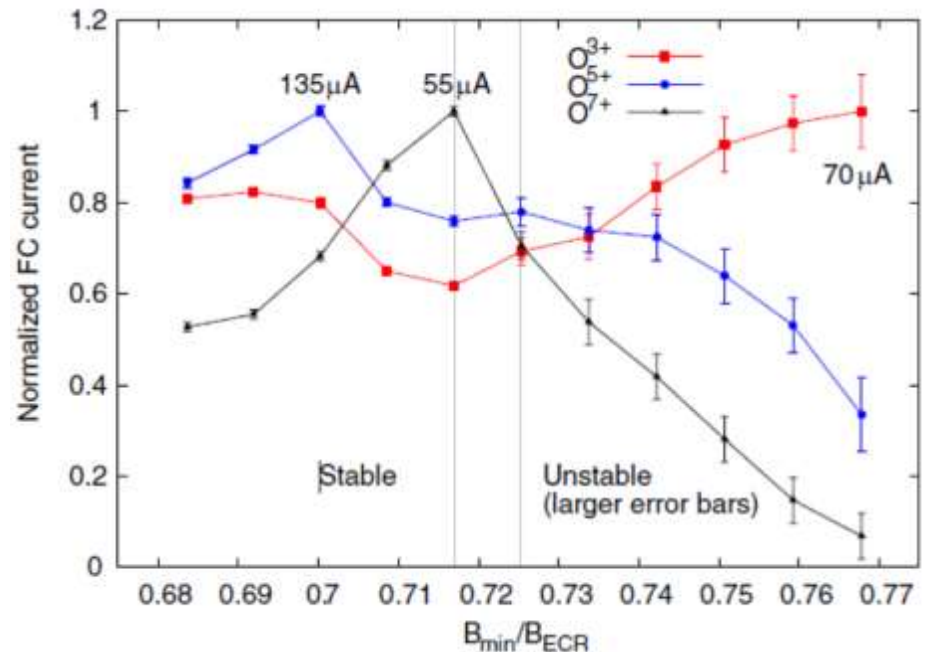
Deviation of ECRIS physics from classical models: experimental evidences

Non linear response of beam current (i.e. plasma density and lifetime) w.r.t. **pumping frequency tuning**



D. Mascali et al., Proc. ECRIS 2010, WECAK02

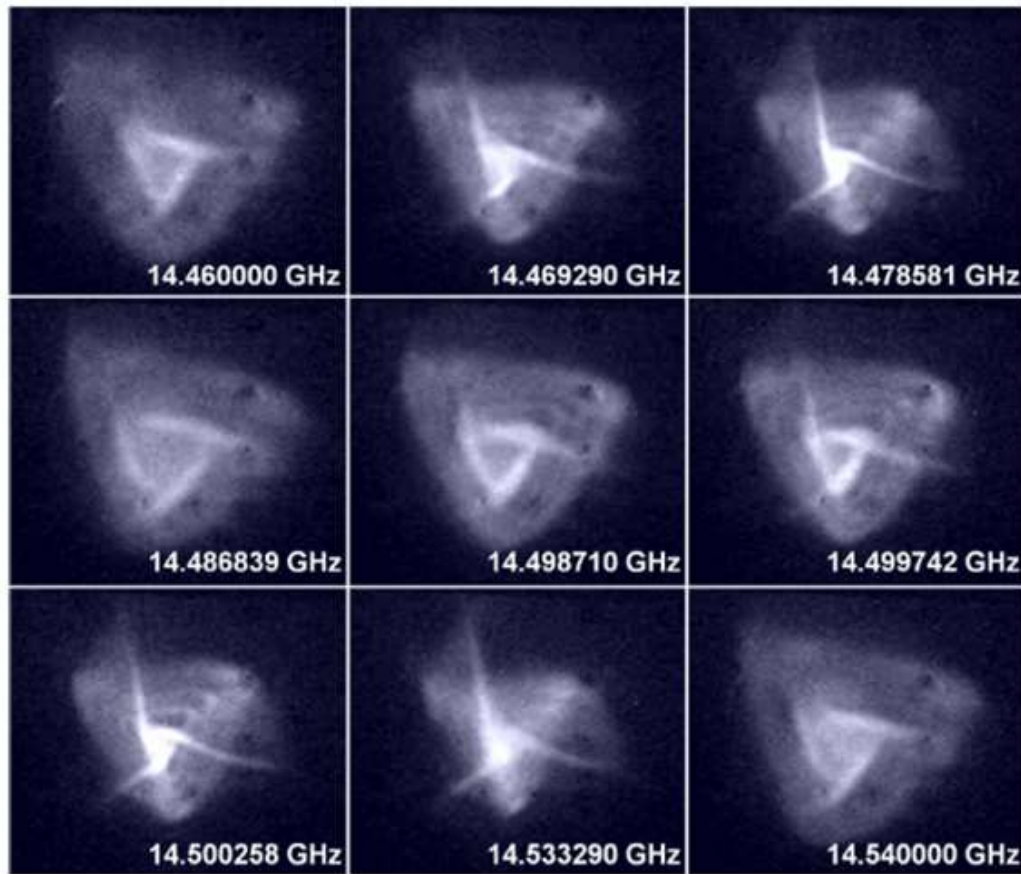
Non linear response of beam current (i.e. plasma density and lifetime) w.r.t. **external magnetic field**



O. Tarvainen et al., PSST 23 (2014) 025020

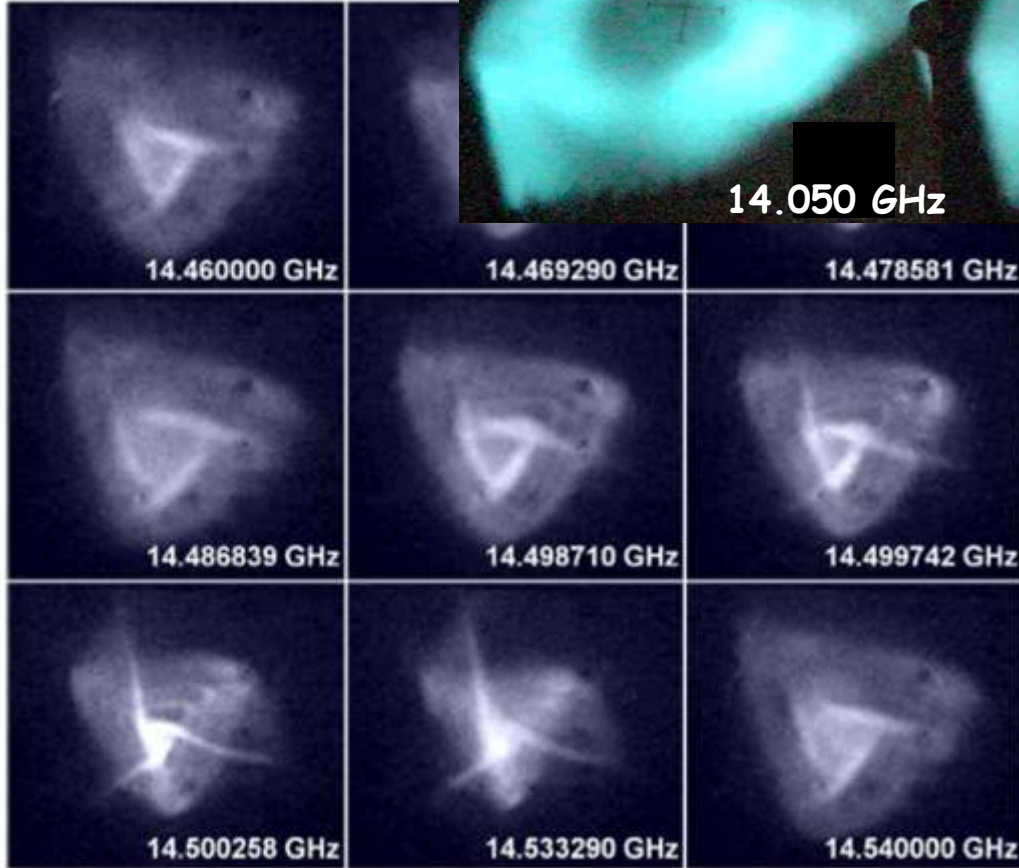
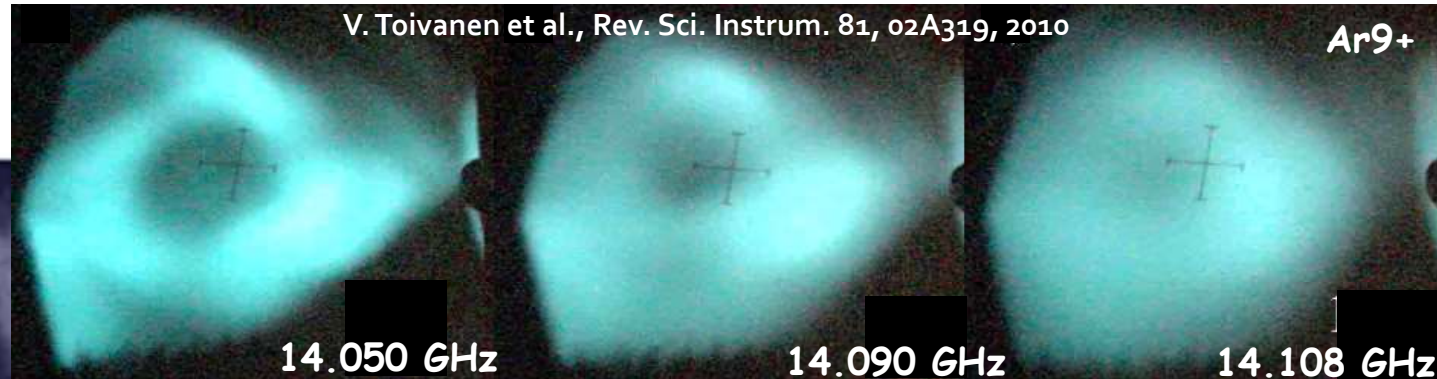
- Variations of few % in the pumping wave frequency or applied magnetostatic field change remarkably the source performances.
- This behaviour is not predicted by the classical model, which requires large scale variations of the frequency (several GHz, not few MHz) or the magnetic field (several kGs)

Interplay between RF and beam formation : experimental evidences



*Viewer 20 cm far from
extraction electrode, NO
optical elements in
between*

Interplay between RF and beam formation : experimental evidences



**Viewer 20 cm far from
extraction electrode, NO
optical elements in
between**

**Other evidences in:
D. Nicolosi et al., MonPE21**

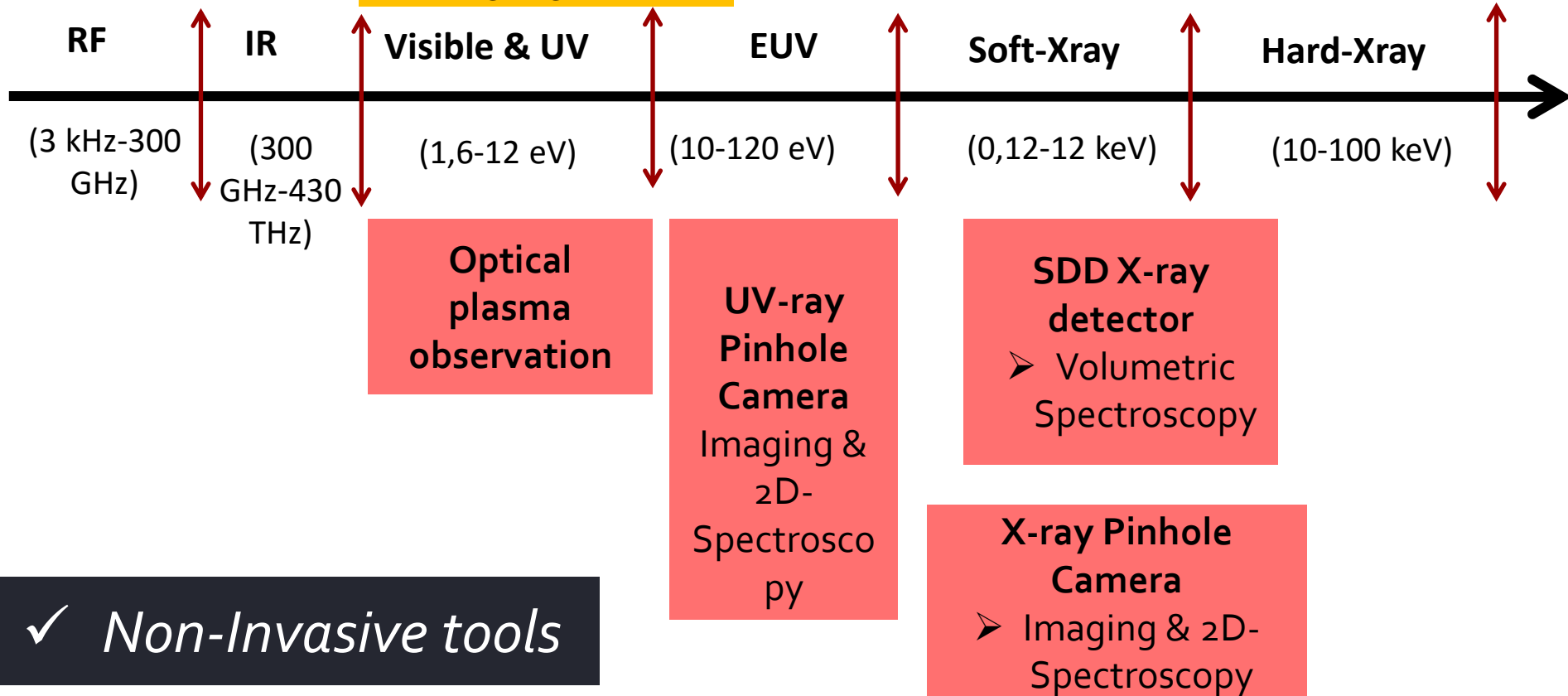
Plasma diagnostics: key physical observables

Spectrum Analyzer

Langmuir Probe

- point by point measurements
- T_e , n_e , EEDF

✓ *Invasive tools*

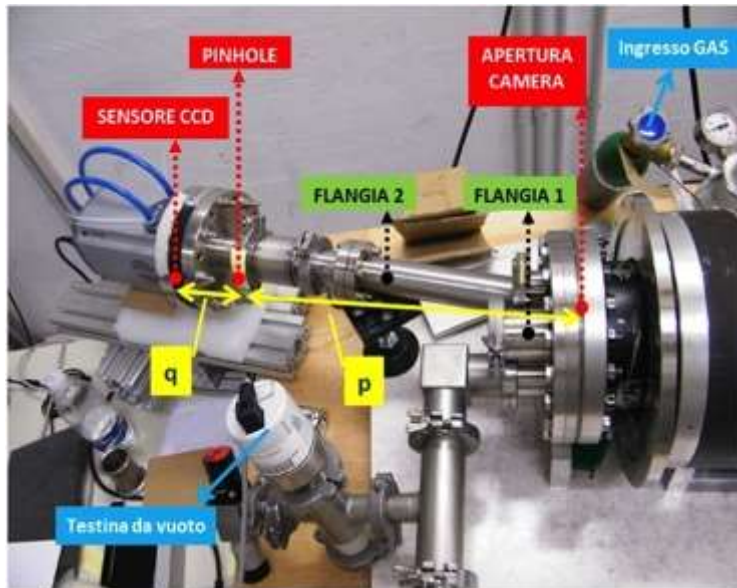


✓ *Non-Invasive tools*

Highlights on...

- Advanced diagnostics tools:
 - **Space and energy resolved X-ray imaging**
 - **Interferometry**
 - **Perspectives**
- Experimental study of the fine tuning effect of magnetic field and pumping wave frequency
- Study and tests of new plasma heating schemes: **Electron Bernstein Waves**
 - Observation and study about plasma waves impact on plasma heating
 - **Stimulated production of plasma waves** for more intense ion beams of light multicharged ions.

Advanced techniques of plasma diagnostics: the X-ray pin-hole camera

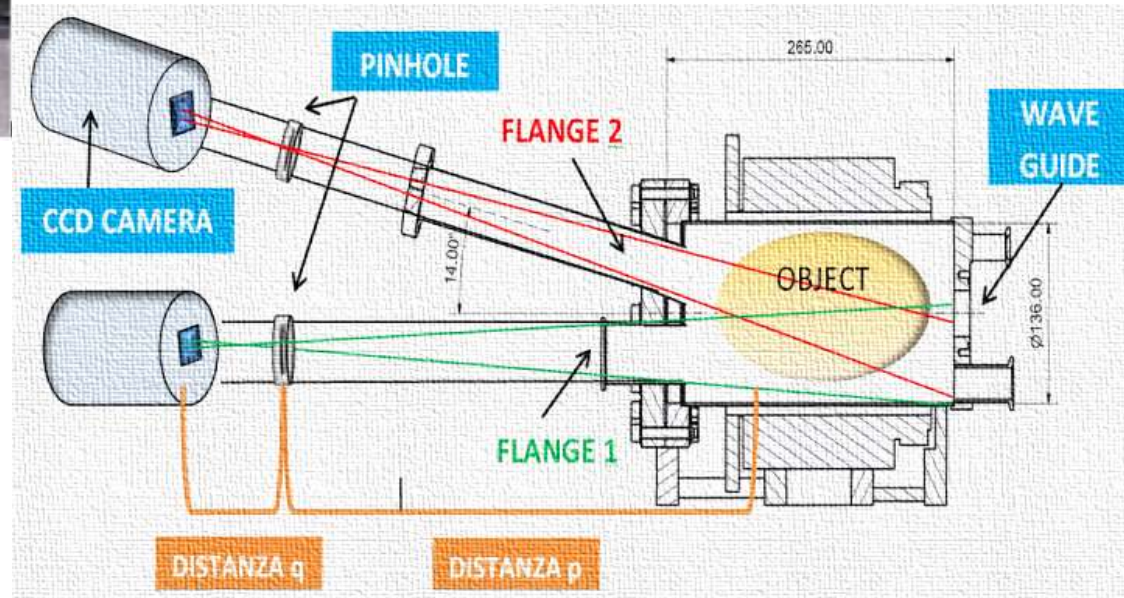


X-ray imaging can be performed with a pin-hole camera technique

The pin-hole is mounted between the plasma and a X-ray sensitive CCD camera having 1024x1024 pixels in the 0.5-15 keV energy domain

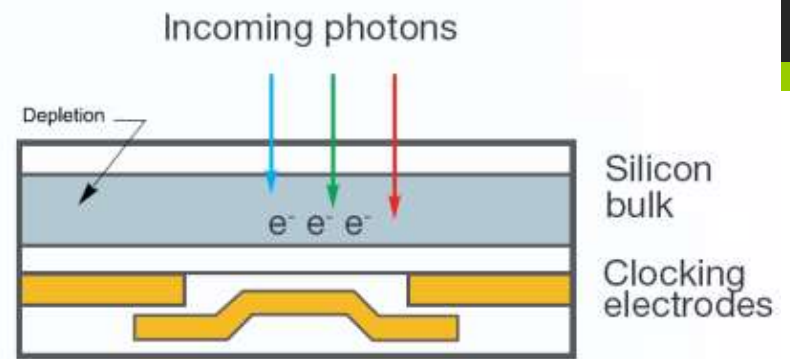


X-ray sensitive CCD - camera

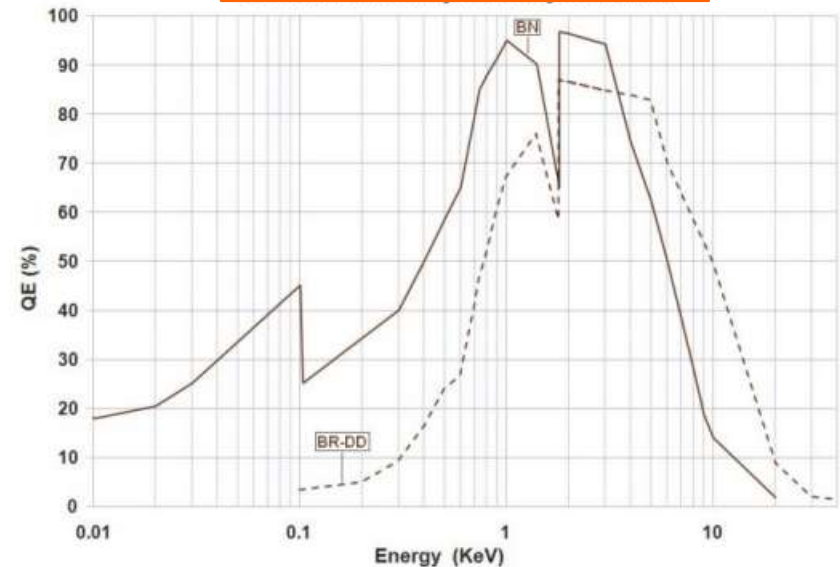


X-ray imaging - CCD camera

Andor, iKon M SO
DO934 – BR-DD



Quantum efficiency curve

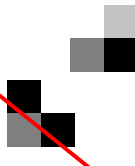


Energy range: 0.1 – 30 keV

- ❑ Silicon Chip of area $13.3 \times 13.3 \text{ mm}^2$ made by a matrix of 1024×1024 pixels
- ❑ Back-illuminated - Deep depletion pixels. **Linear response 99%.**
- ❑ Peltier's cell for cooling (-100°C by water recycling)
- ❑ $25\mu\text{m}$ Be removable window for visible light suppression.



CCD camera – images analysis

1. A single photon can excite a group of pixels, the pixel with the maximum intensity represent the impinging position of the photon, but the energy can be distributed in the neighbouring pixels.
2. Energy reconstruction algorithm was developed to recognise pixels with the maximum intensity and correlated ones, photons with overlapping clouds are recognized and discharged because energy can not be reconstructed. A diagram illustrating overlapping pixel clouds. It shows a grid of pixels with varying intensities (shades of gray). A red diagonal line is drawn across the grid, indicating that photons with overlapping clouds are recognized and discharged because energy cannot be reconstructed.
3. The out-coming images, obtained summing thousands of frames, are spatially and energetically resolved.

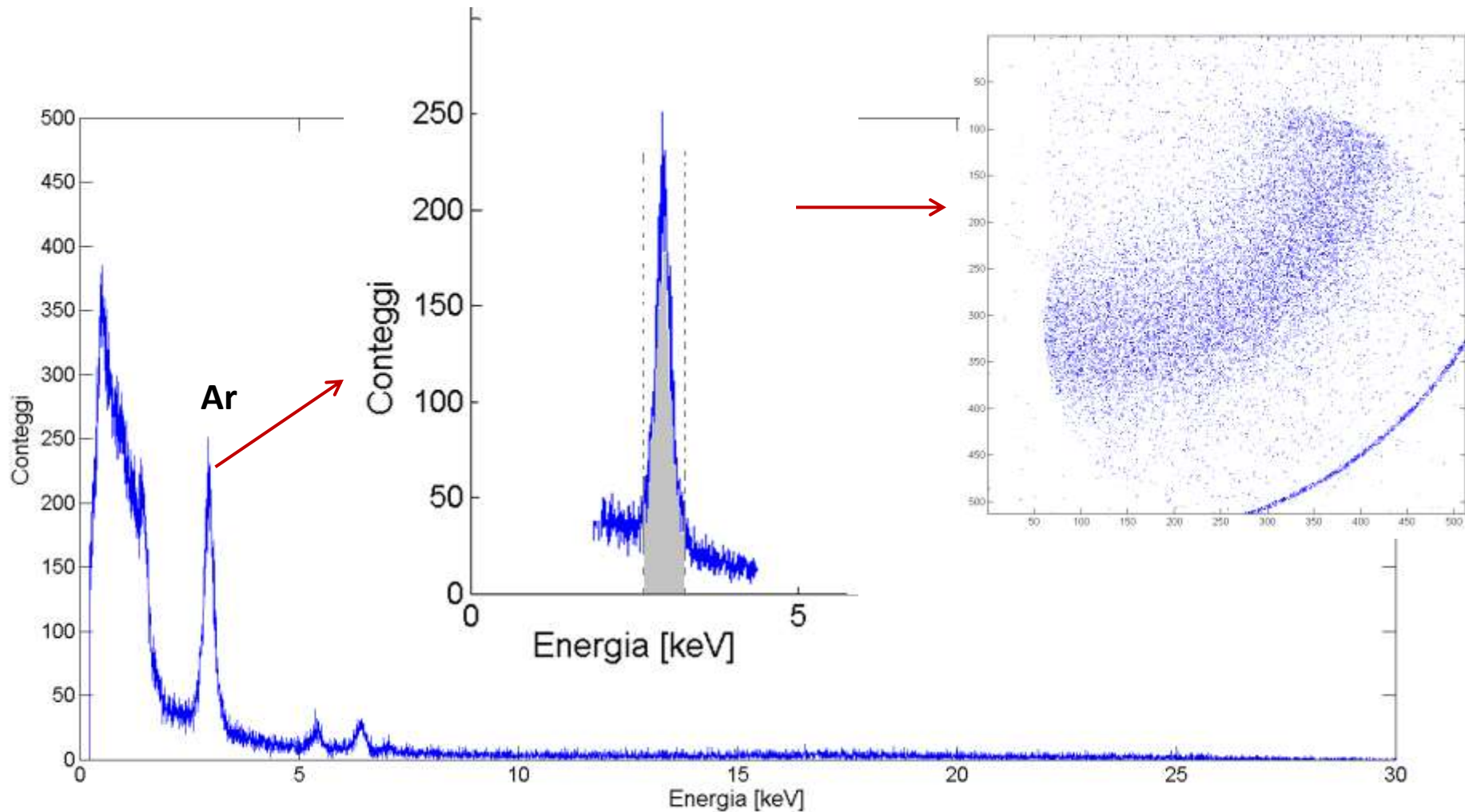
Excellent energy resolution

137 eV@Fe-K α

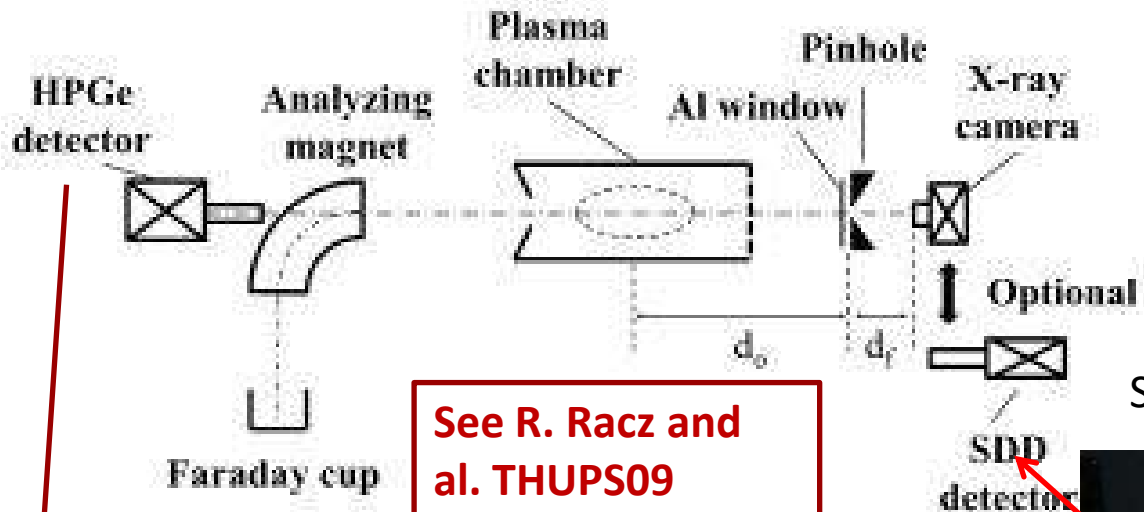
Space resolved spectroscopy



Selection of fluorescence lines for the extrapolation of the various elements displacement into the plasma → **selection of the lines**

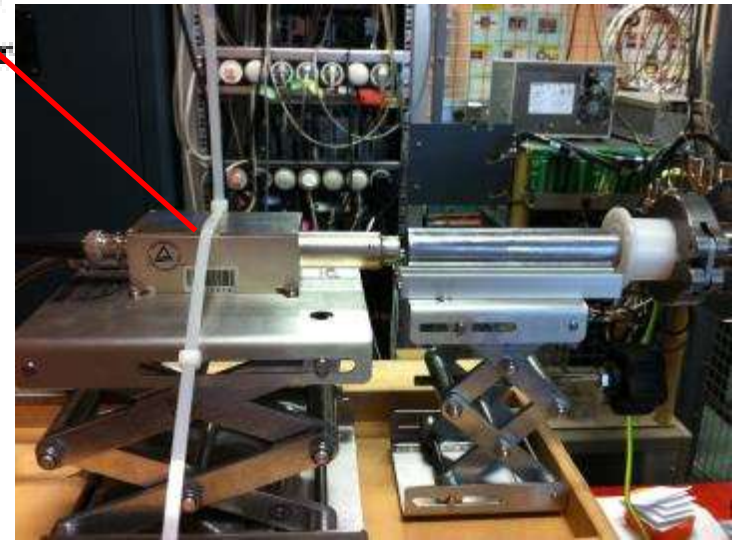


Setup for X-ray spectroscopy at ATOMKI



See R. Racz and al. THUPS09

Silicon Drift Detector ($2 < E < 30 \text{ keV}$)

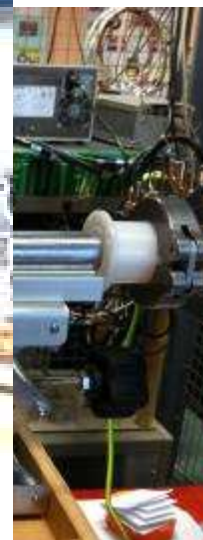


Setup for X-ray spectroscopy at ATOMKI

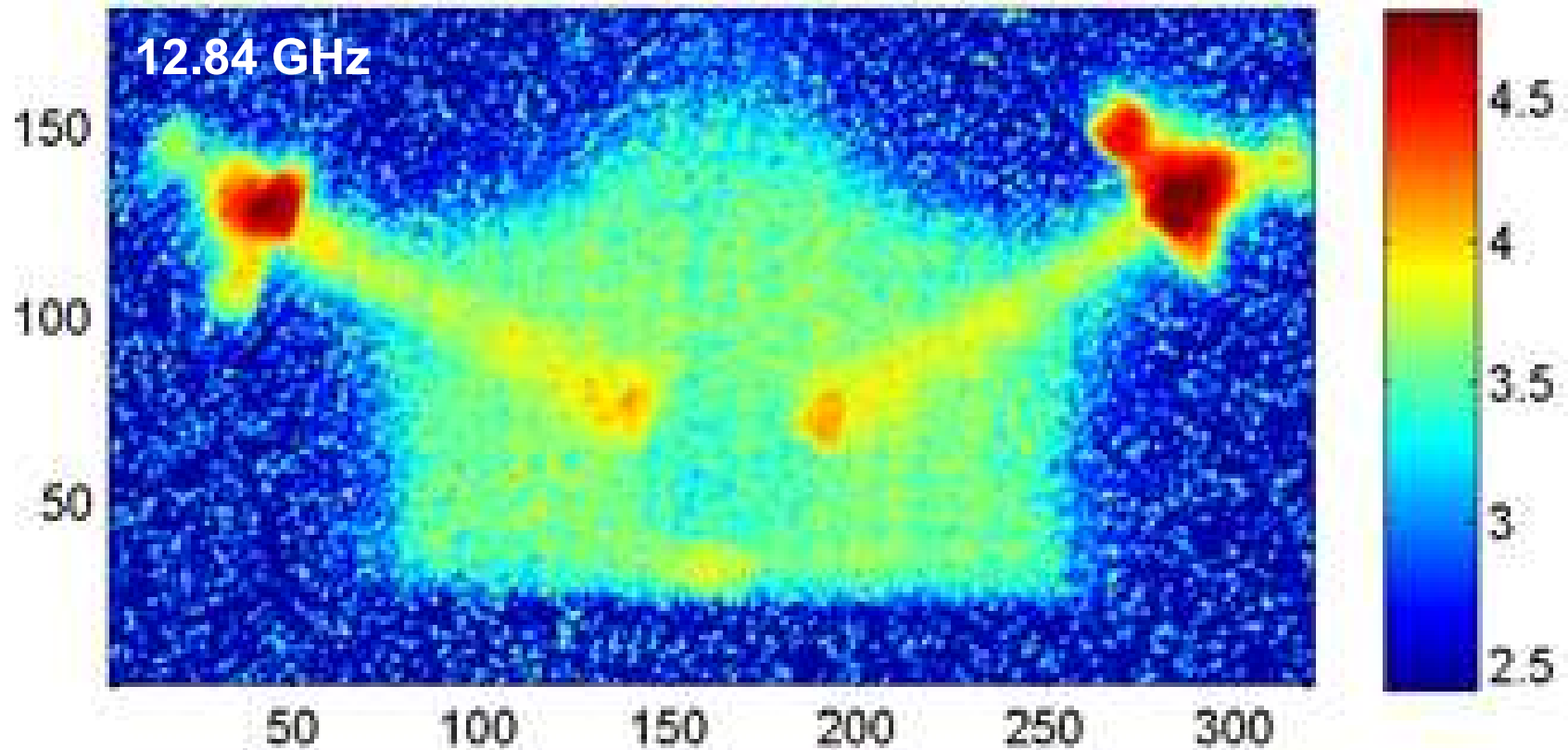
HPGe
detector



($E < 30 \text{ keV}$)

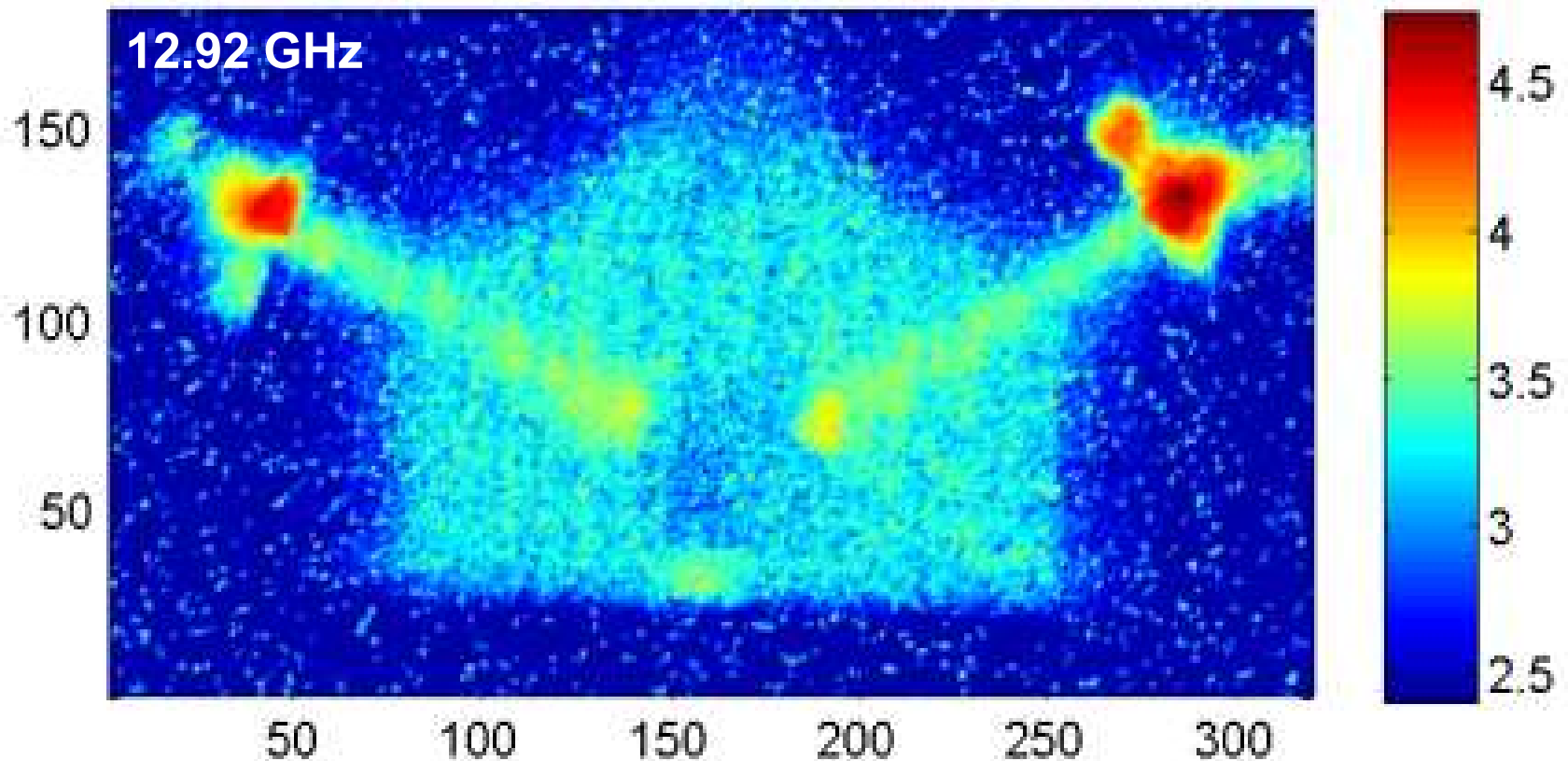


INFN-ATOMKI experiment : 2D plasma imaging @ 12.84 GHz



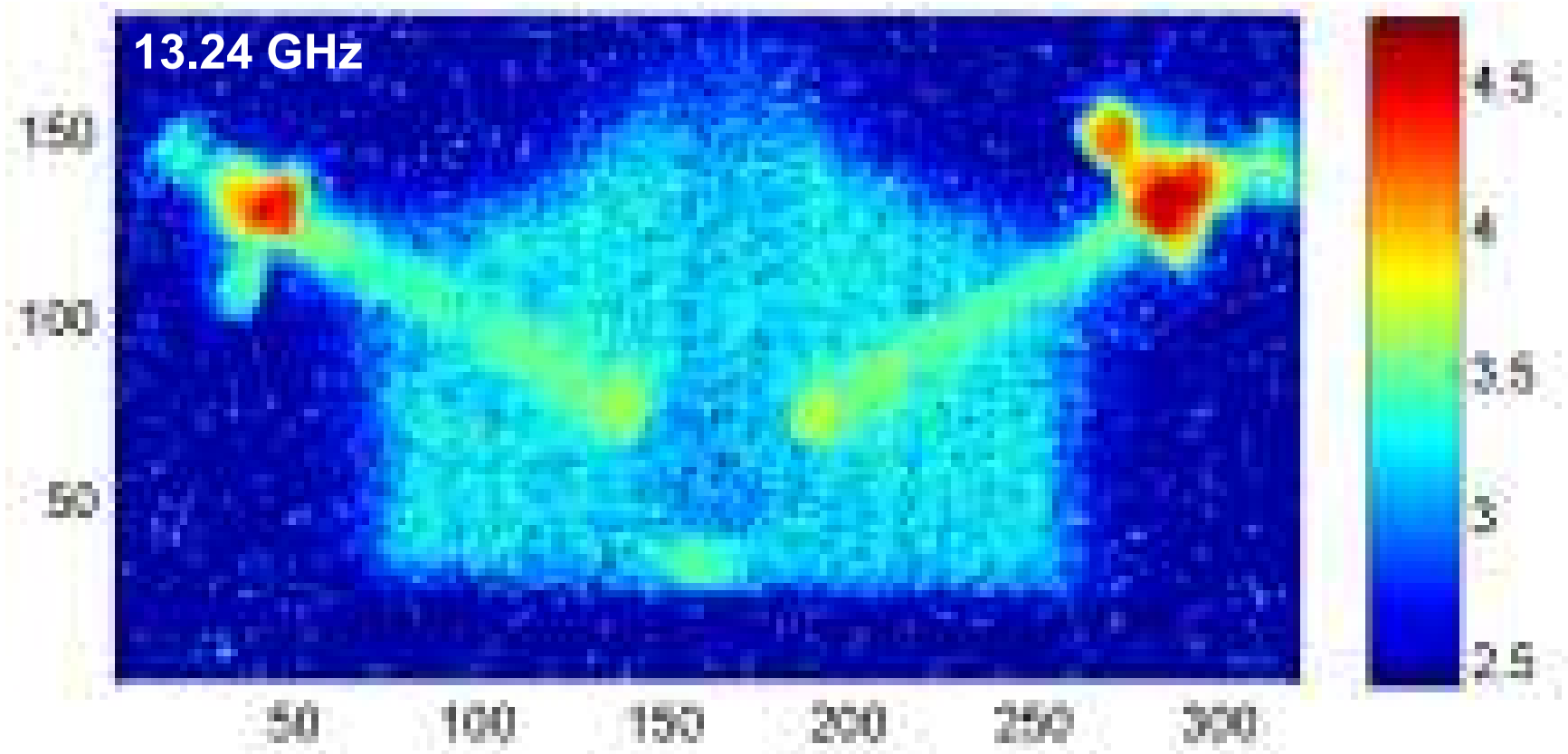
LOG SCALE 10^x

INFN-ATOMKI experiment : 2D plasma imaging @ 12.92 GHz



LOG SCALE 10^x

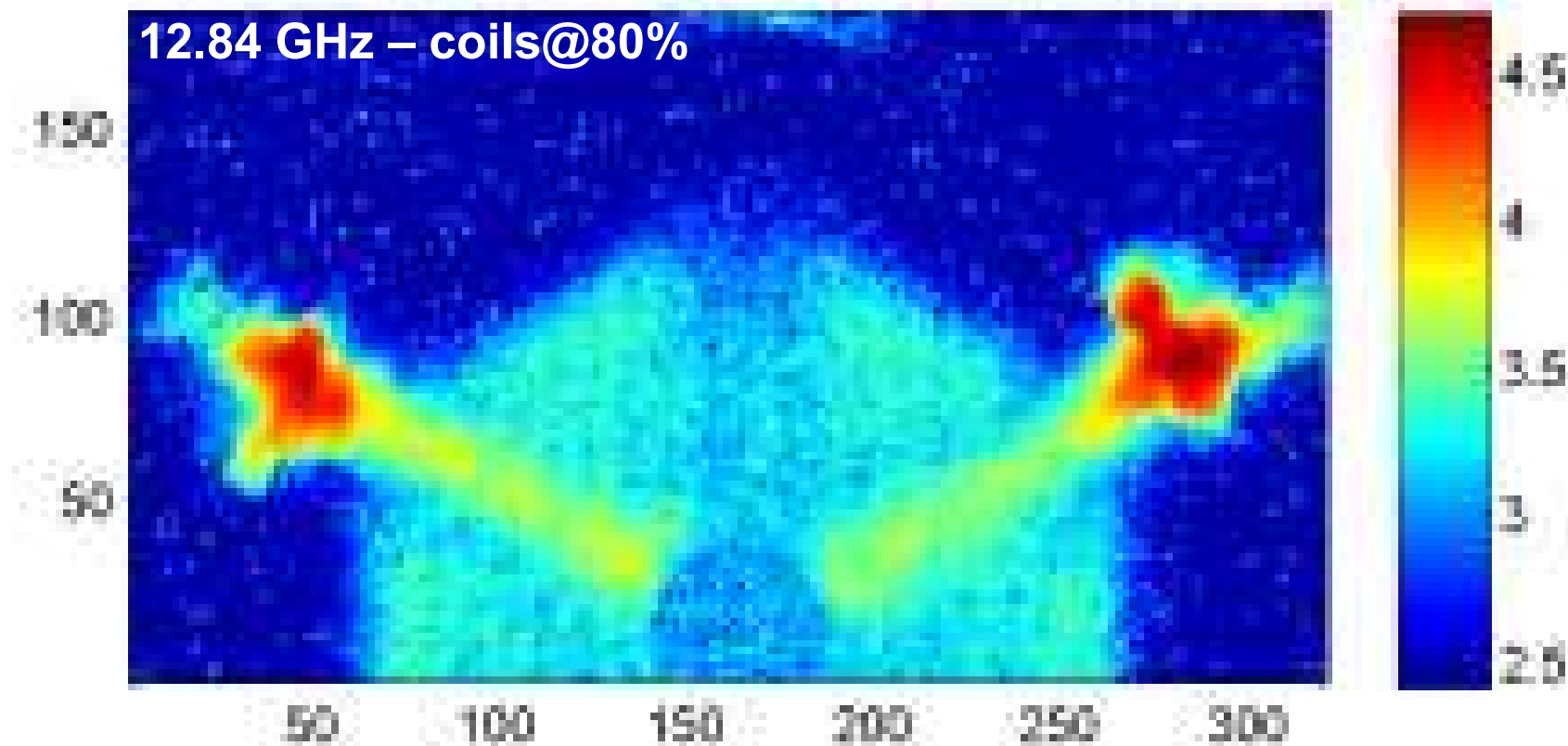
INFN-ATOMKI experiment : 2D plasma imaging @ 13.24 GHz



LOG SCALE 10^x

INFN-ATOMKI experiment : 2D plasma imaging @ 12.84 GHz

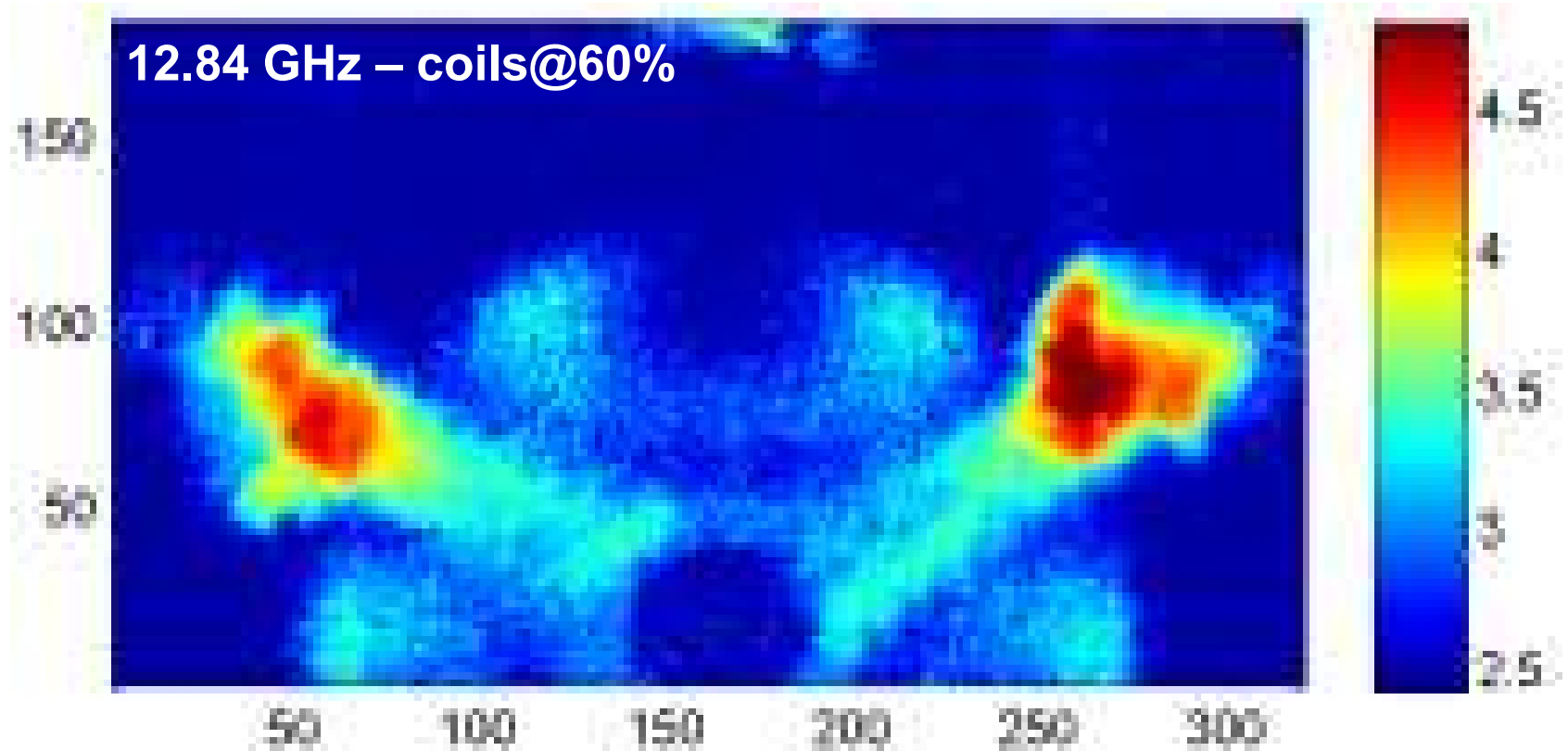
COILS @ 80%



LOG SCALE 10^x

INFN-ATOMKI experiment : 2D plasma imaging @ 12.84 GHz

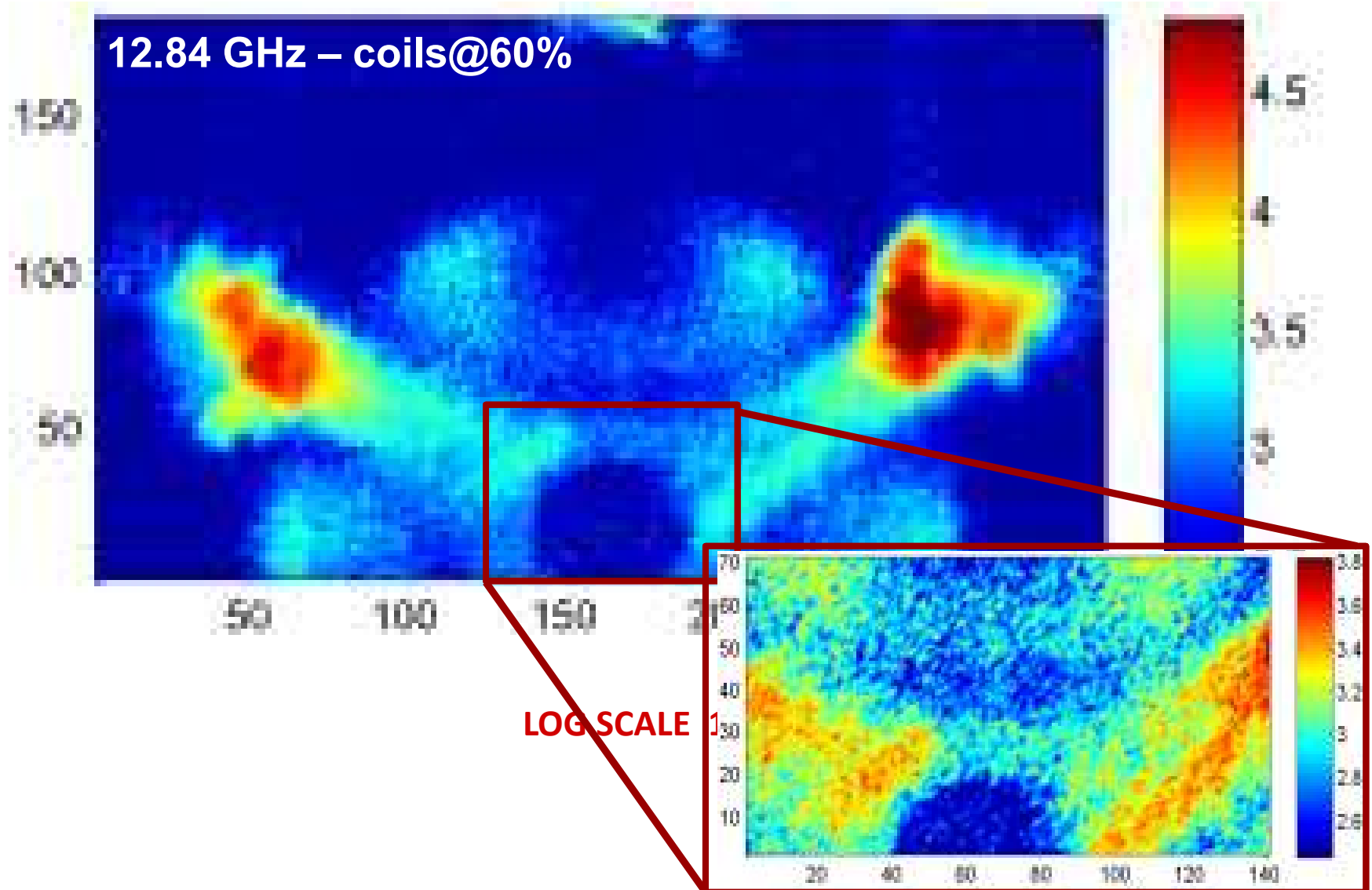
COILS @ 60%



LOG SCALE 10^x

INFN-ATOMKI experiment : 2D plasma imaging @ 12.84 GHz

COILS @ 60%





Some Comments...

- RF frequency has a deep impact not only on plasma heating rapidity, but on the WHOLE PLASMA STRUCTURE.
- Frequency and magnetic field fine regulations are needed to optimize current, charge states and emittance.
- Strong correlation of n_e, T_e, t_i to define HCl buildup and beam emittance formation
- Future machines NEEDS to have a *microwave absorption oriented design*

**See D.Mascali et al.
WED M07**



Stimulated production of plasma waves

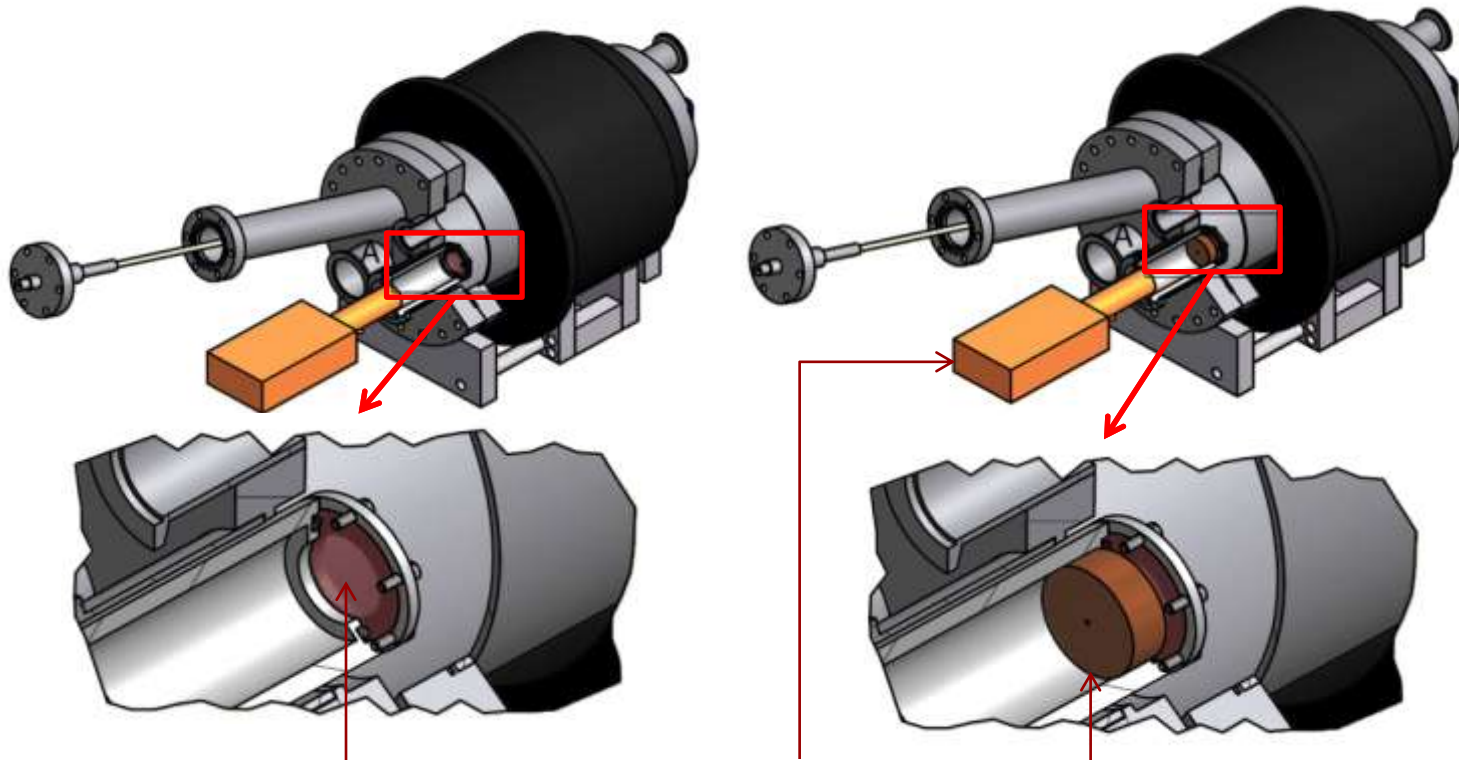
Formation of Overdense plasmas in simplified magnetic structures

- ***Possibility of simplifying magnetic structures for multi-charged ion production***
- ***Large amounts of X-rays generation and cutoff density overcoming***

1. **Overdense plasma generation**
2. **Formation of a suprathermal electron component**
3. **Non-linear broadening of the spectrum of the pumping electromagnetic wave**

1. **Electrostatic “plasma-immersed” probe (Langmuir probe)**
2. **X-ray “volume” spectroscopy made with HpGe and SDD detectors**
3. **X-ray spatial and energetic resolved spectroscopy**
4. **Small-wire plasma-immersed antenna connected to a Spectrum Analyzer**

Plasma wave formation is highlighted by X-ray emission: Setup for X-ray spectroscopy



8 μ m kapton window

SDD –detector by KETEK

25 micron Be windows (*very low efficiency @1-2keV*)

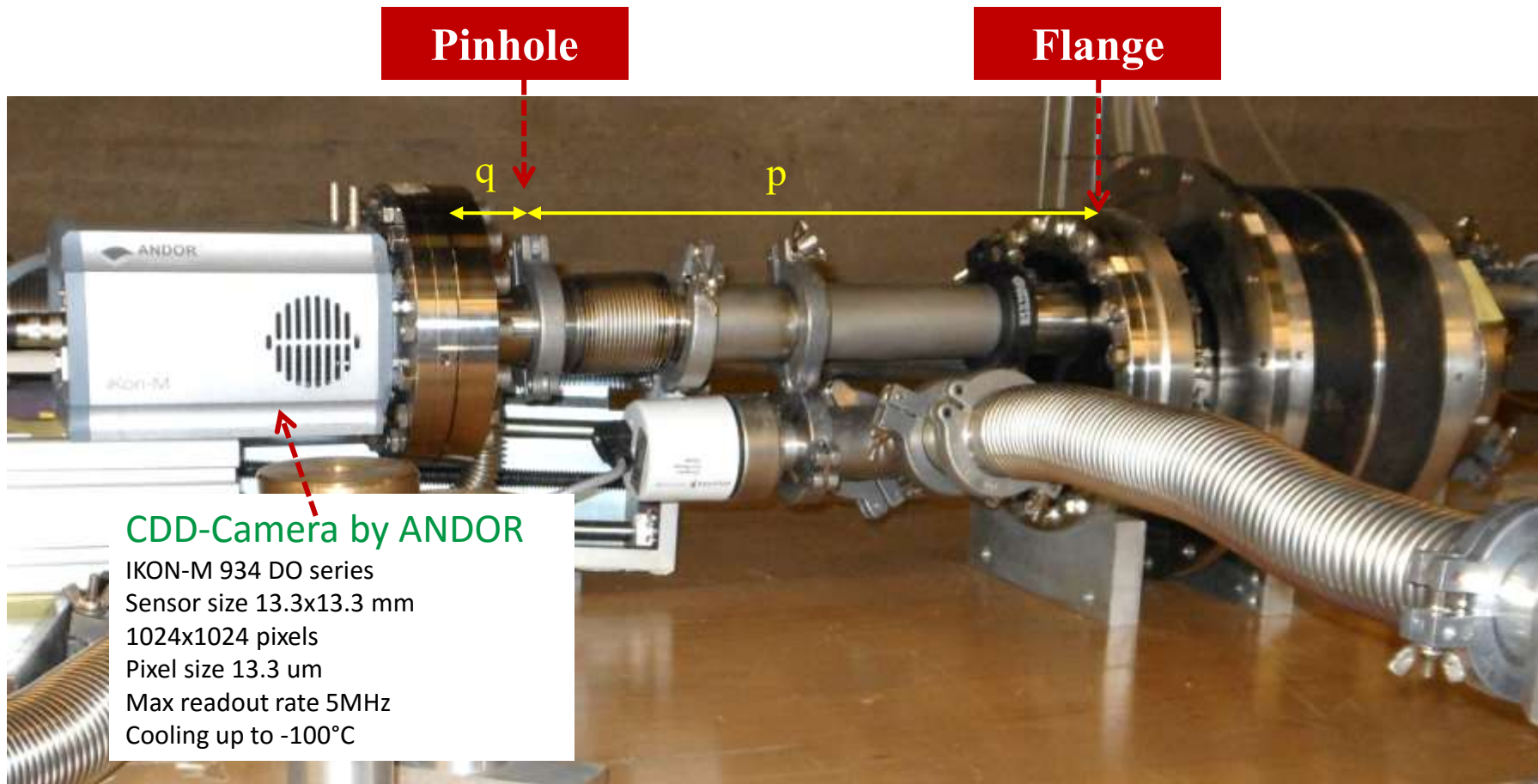
80 mm² active surface

160 eV @ 5.9 keV

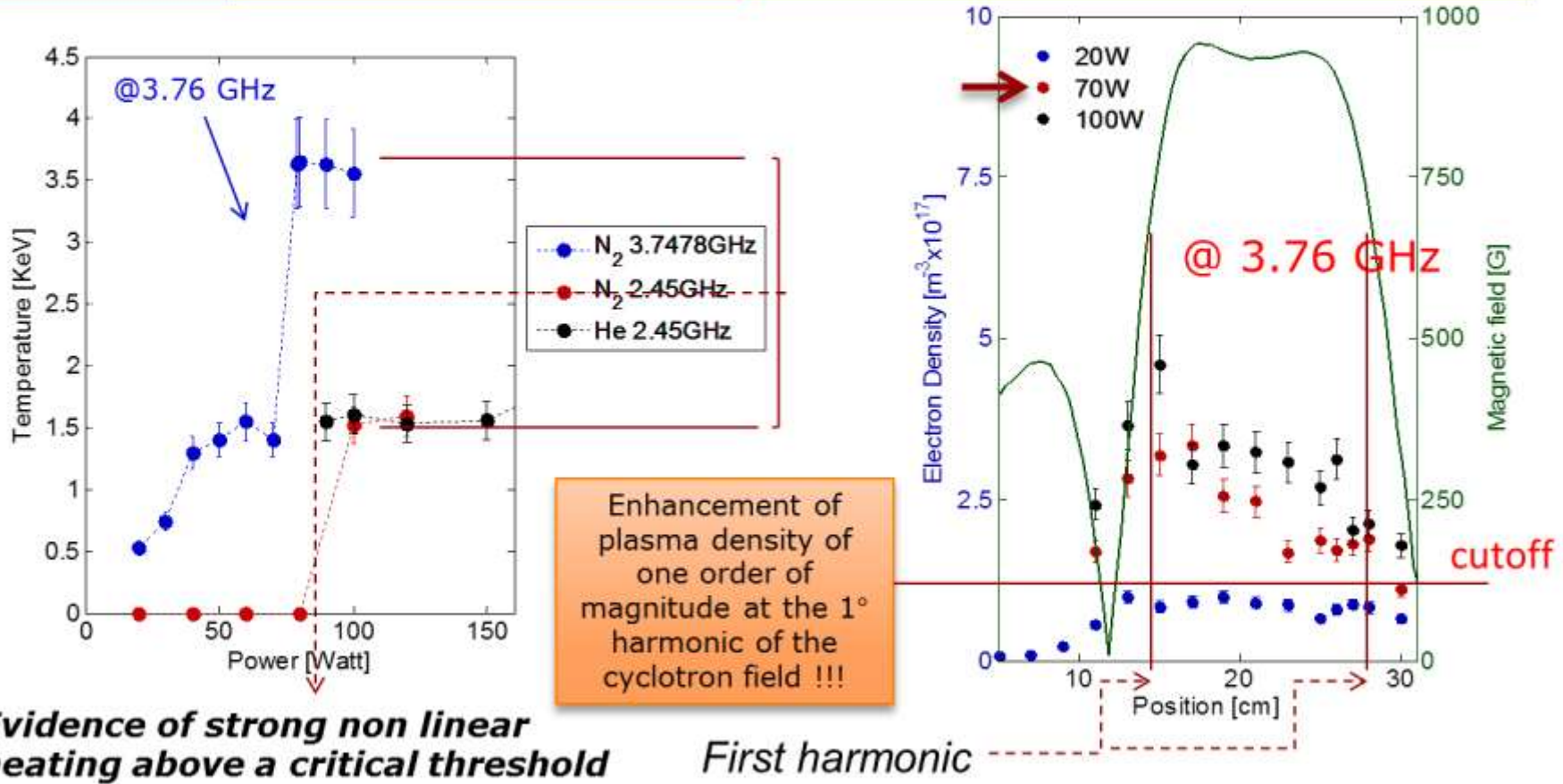
Operative conditions: up to 500 kcps at 2.1 usec. peaking time

0.7 mm² collimator

Setup for X-ray imaging on Plasma Reactor



The non linear transition of electron temperature and the cutoff density overcoming confirm that plasma modes were formed



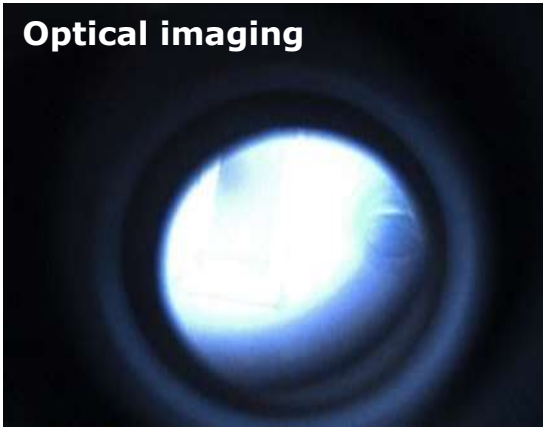
Evidence of strong non linear heating above a critical threshold

First harmonic

Experimental observation shows a non-linear growing of plasma temperature and density, with a JUMP above a certain threshold of the RF power.

First direct observation of a Hot Electron Layer in off-resonance discharge

Optical imaging



Images in the optical window evidence the generation of a high-brightness annulus surrounding a dark hole.

X-ray imaging evidences that the pumping power is deposited in the annulus, where the energetic electrons are generated

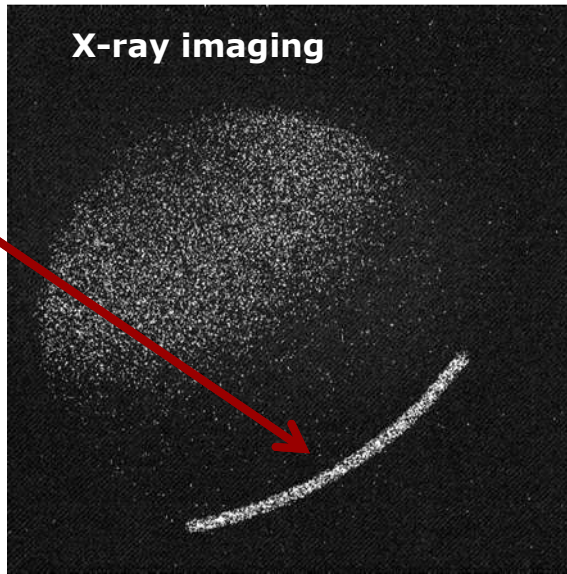


Transversal reconstruction of the plasma structure in X-ray domain (1-30 keV).

Plasma chamber

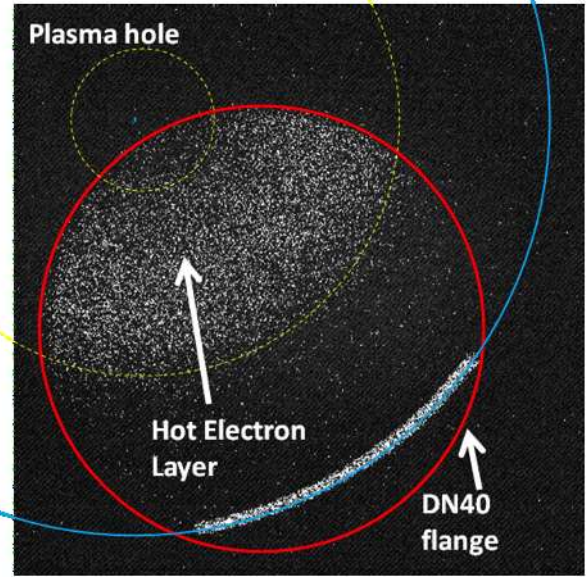
A high brightness strip appears due to electrons impinging on the chamber walls

X-ray imaging



gas: Argon
pressure: $3 \cdot 10^{-4}$ mbar
RF power: 100W
100 frames -
1sec exposure for each one

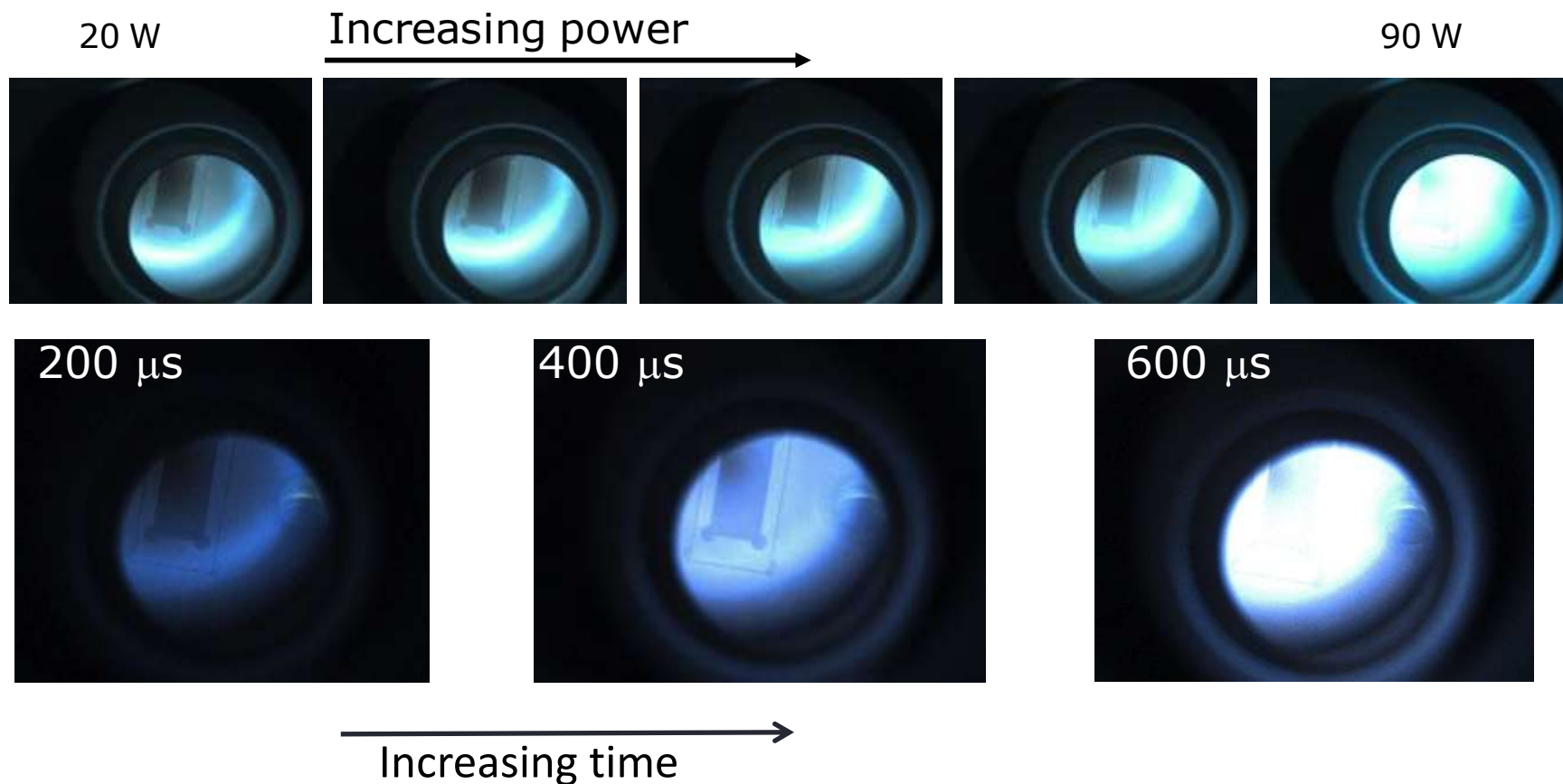
Plasma hole



Hot Electron Layer

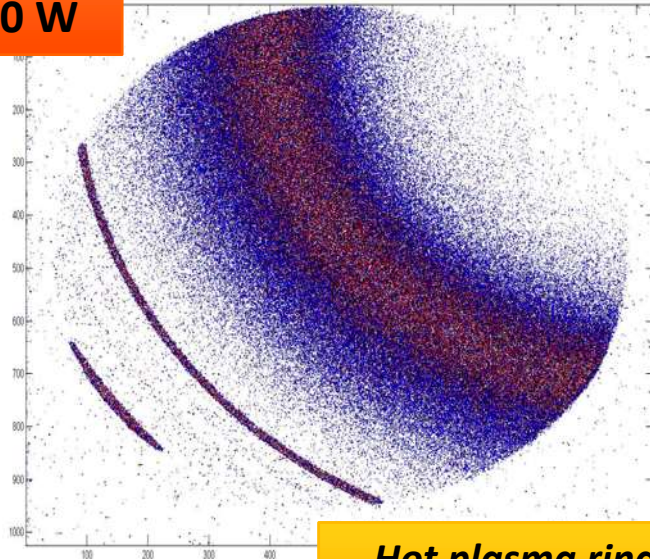
DN40 flange

First direct observation of a Hot Electron Layer in off-resonance discharge



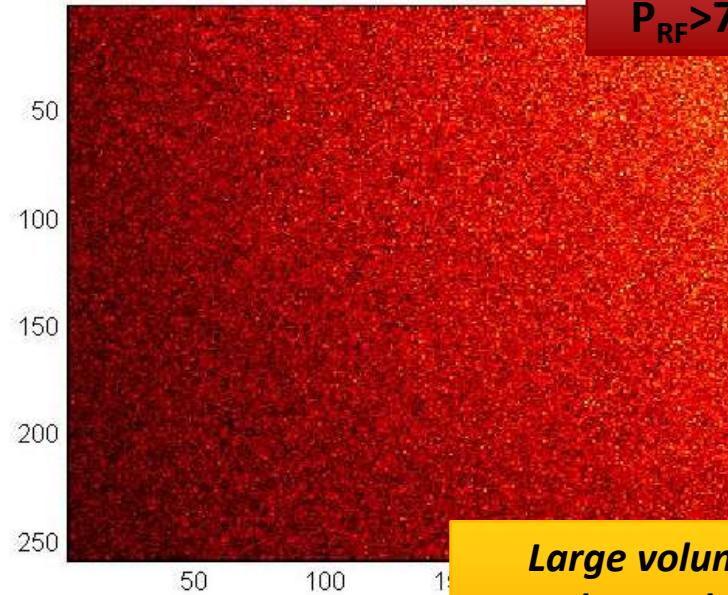
Two different configurations of the plasma: hot ring and plasma hole

$P_{RF} < 70$ W



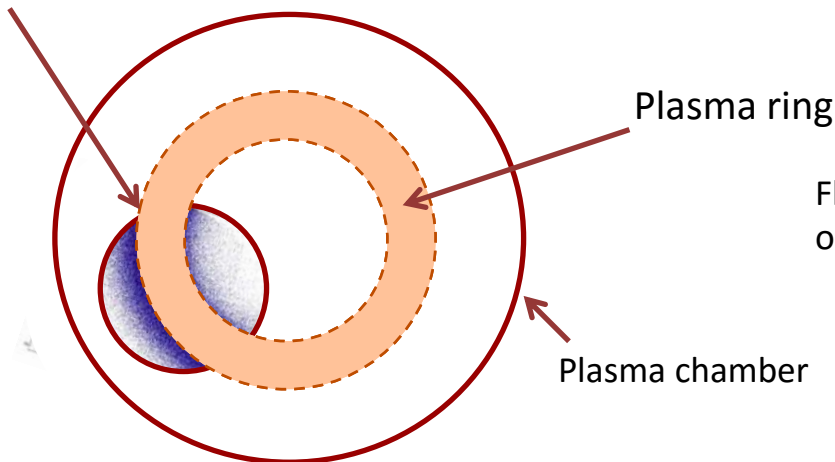
Hot plasma ring

$P_{RF} > 70$ W

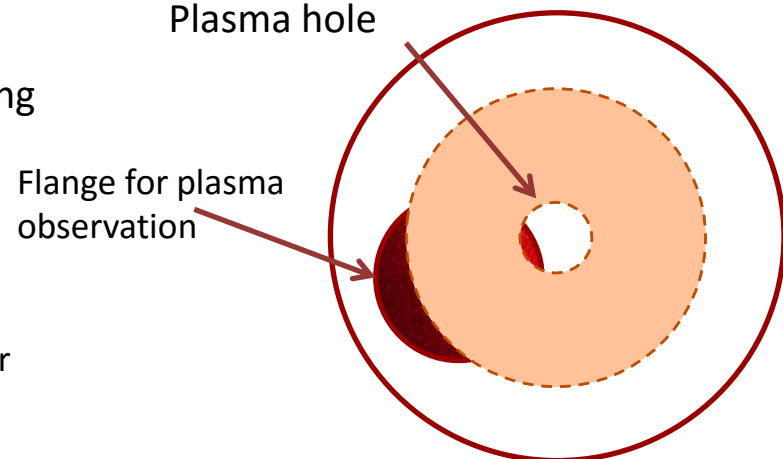


Large volume overdense plasma

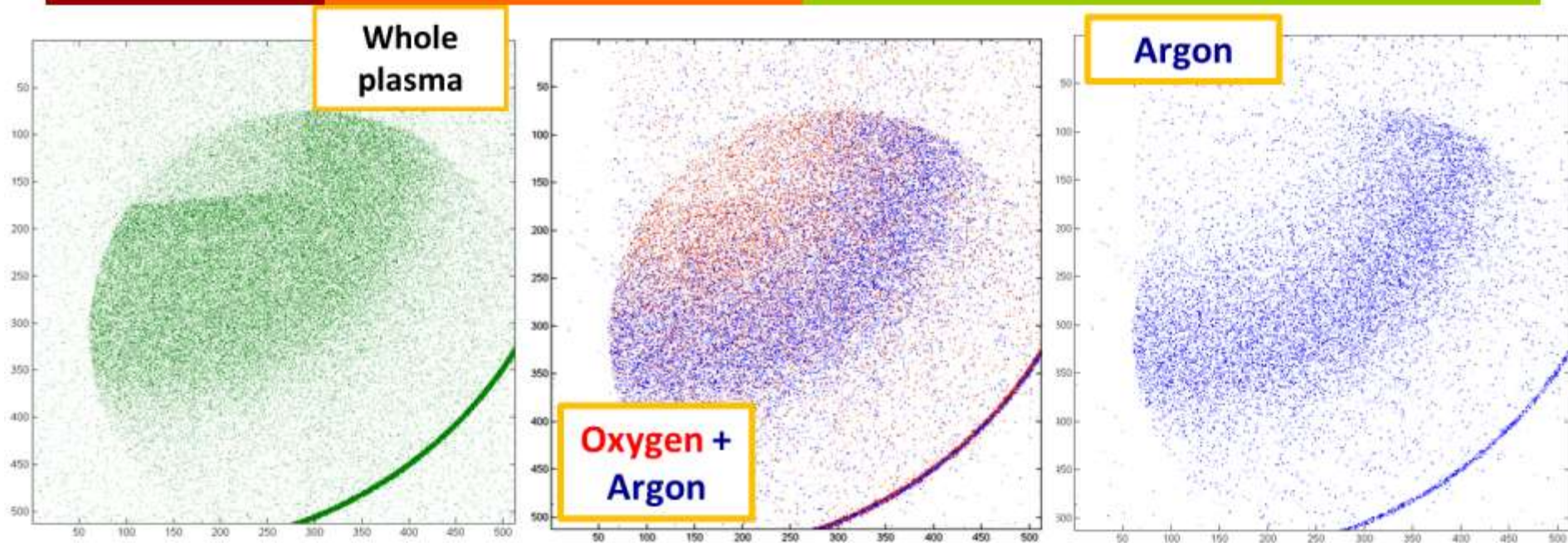
Flange for plasma observation



Plasma hole



Space resolved spectroscopy

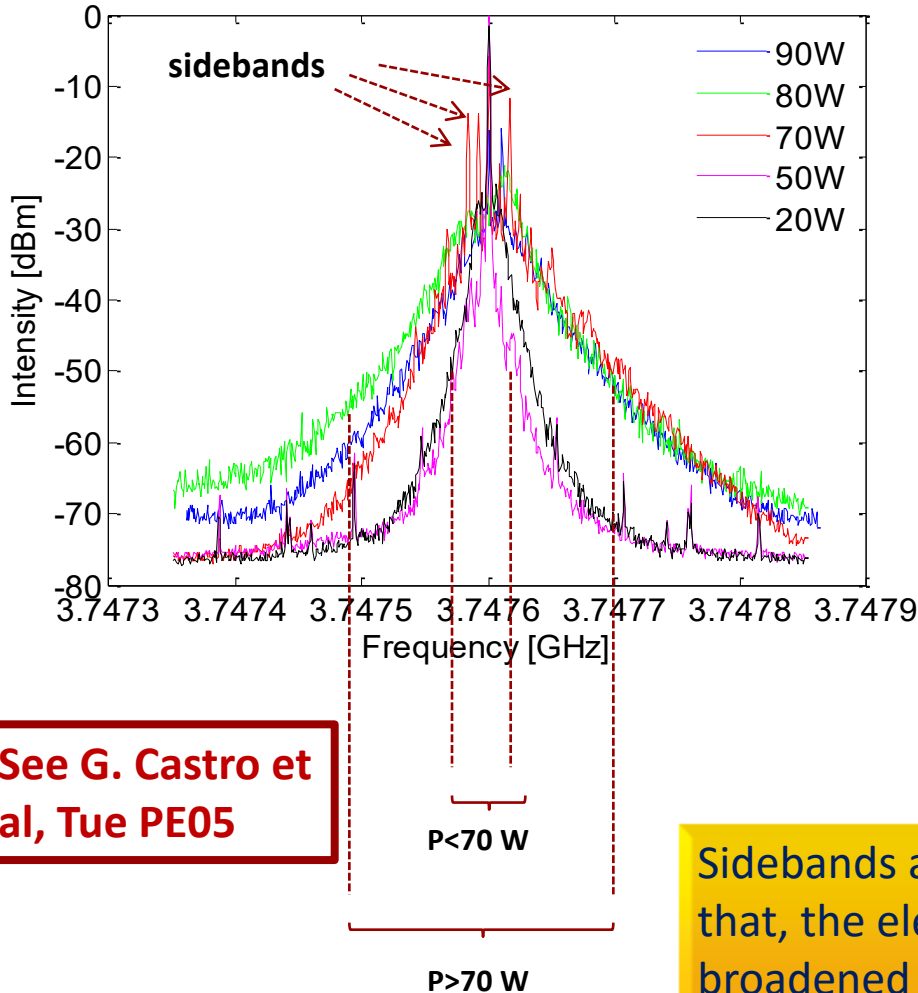


The gas mixing operations highlight the different displacement of different species into the plasma. In particular, **heavier species like Argon are placed at larger radii with respect to the Oxygen**, which concentrates in near axis region.

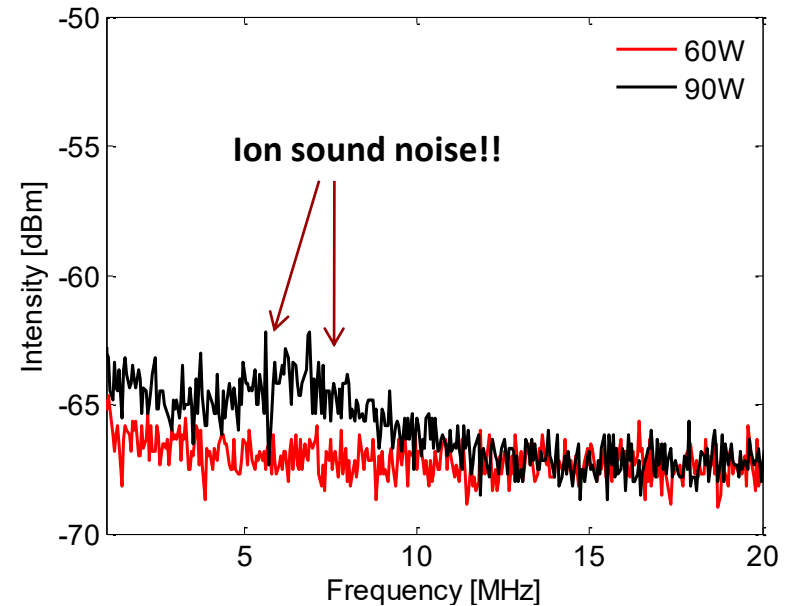
Experimental setup:

Mixture of **Air+Argon** Plasma @ Pressure: **$1.5 \cdot 10^{-4}$ mbar**, RF power: **100 W**

Non linear spectrum broadening



See G. Castro et al, Tue PE05

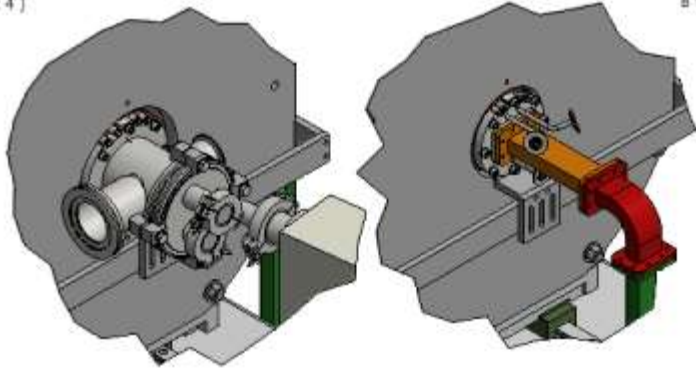


The spectral broadening of the pumping wave is accompanied by the ancillary generation of ion acoustic waves (IAW) in the MHz range

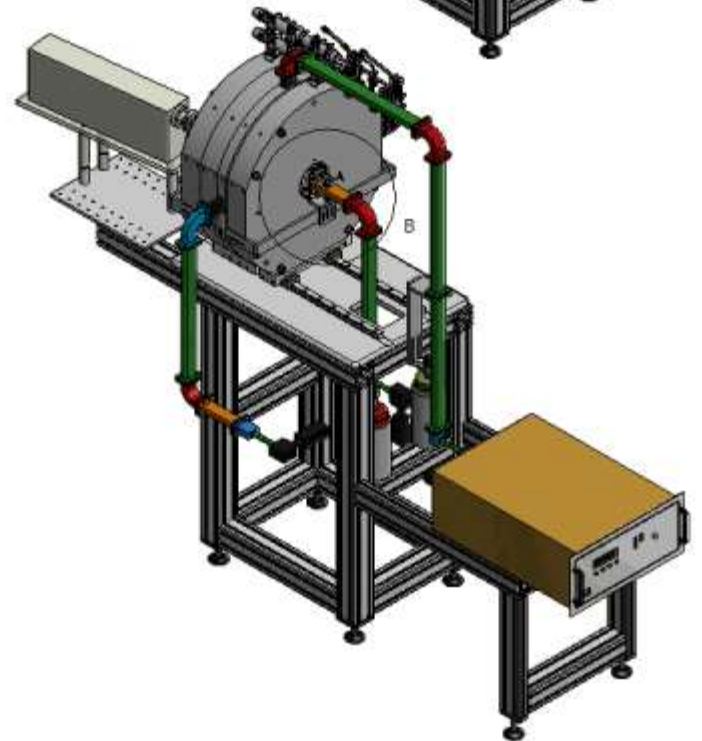
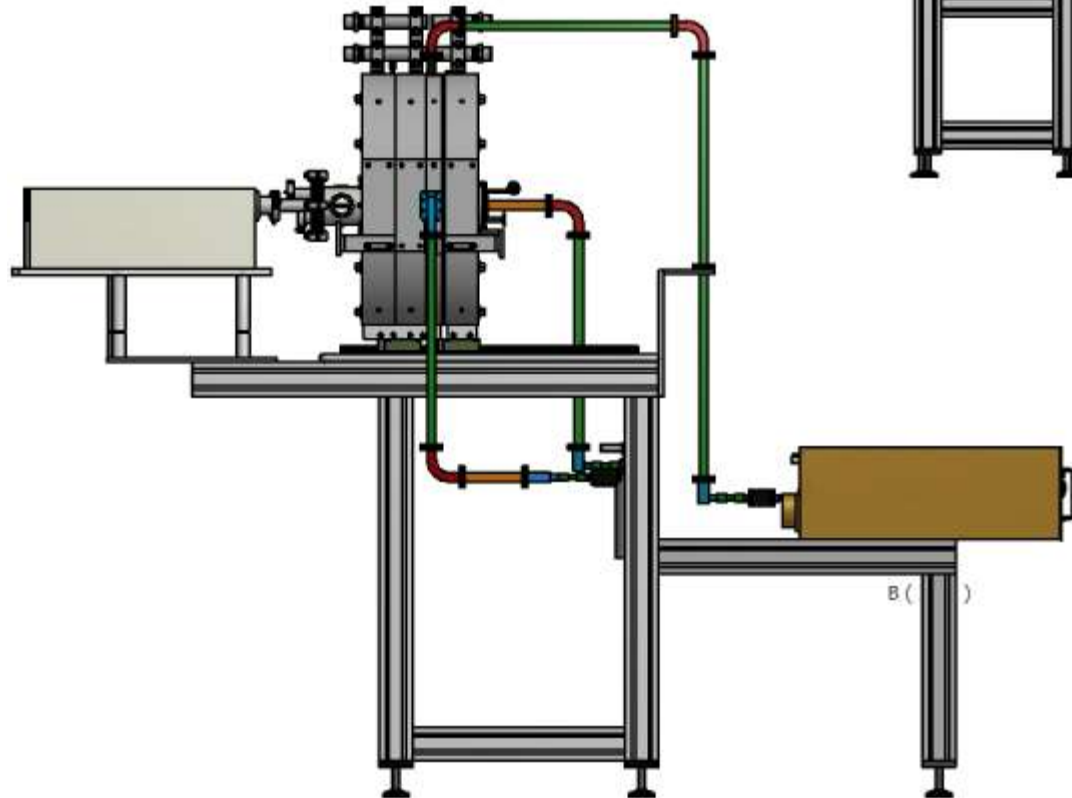
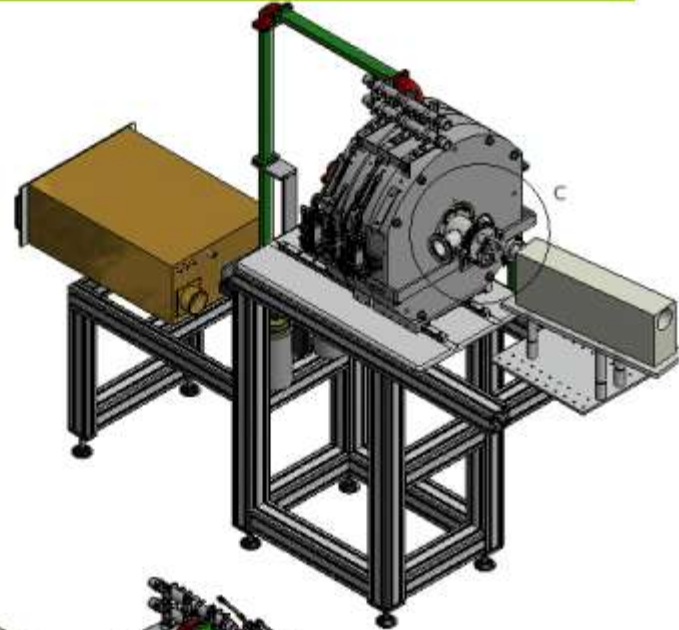
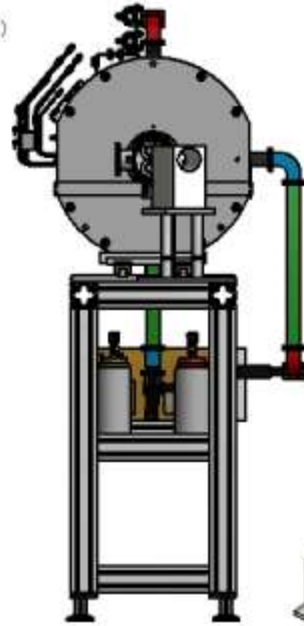
Sidebands appeared at the threshold (70 W). After that, the electromagnetic spectrum was completely broadened by the plasma turbulence.

Flexible Plasma Trap

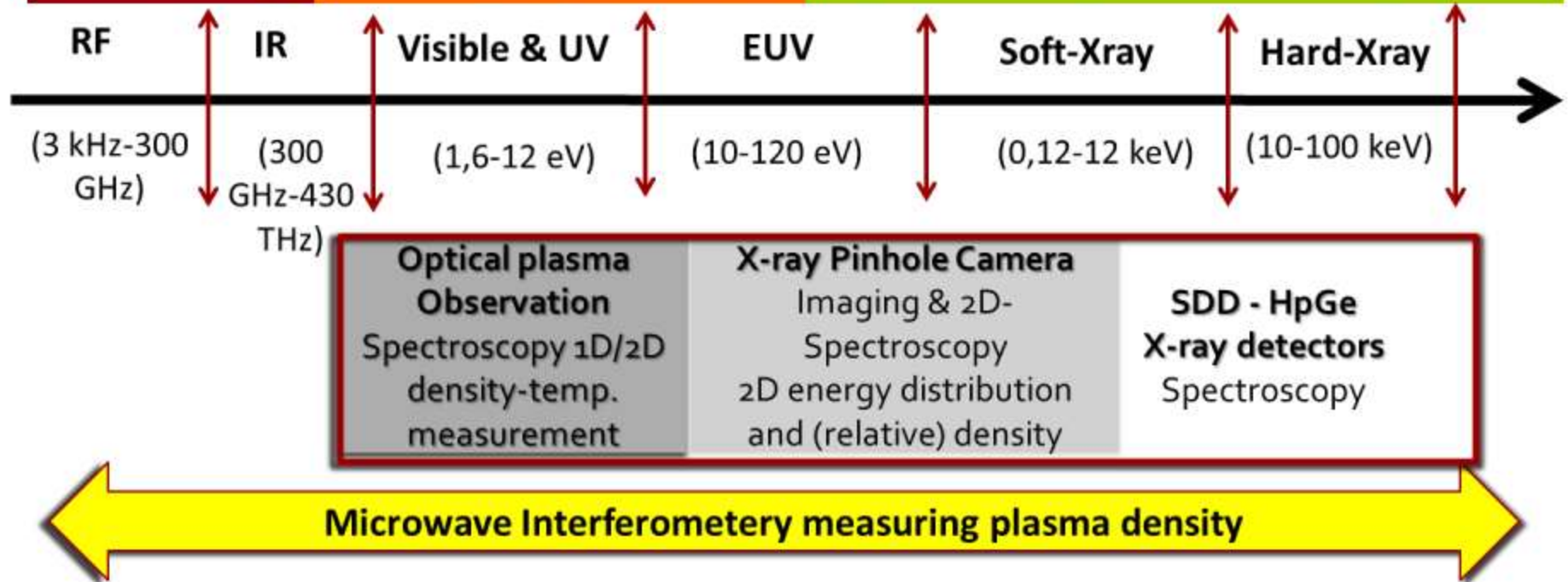
(1:4)



B (1:4)



Plasma Diagnostics: *sophisticated tools for covering the entire EM spectrum*



We need a tool able to measure density of electrons with an externally injected "probing" radiation (no perturbation since $P_{\text{probing}}/P_{\text{exciting}} < 1\%$)

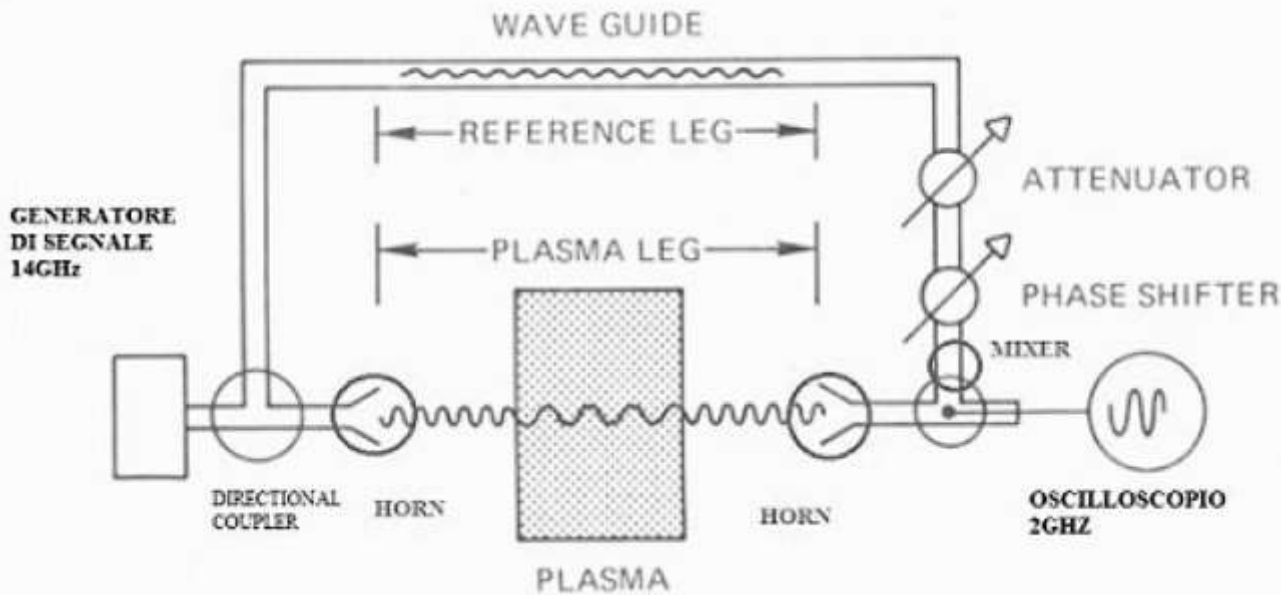
Density measurement technique no-longer based on plasma emission but on "response-on-transmission" of microwaves through the plasma



MICROWAVE INTERFEROMETRY



Classical interferometry for plasmas



Classical Scheme of Interferometer

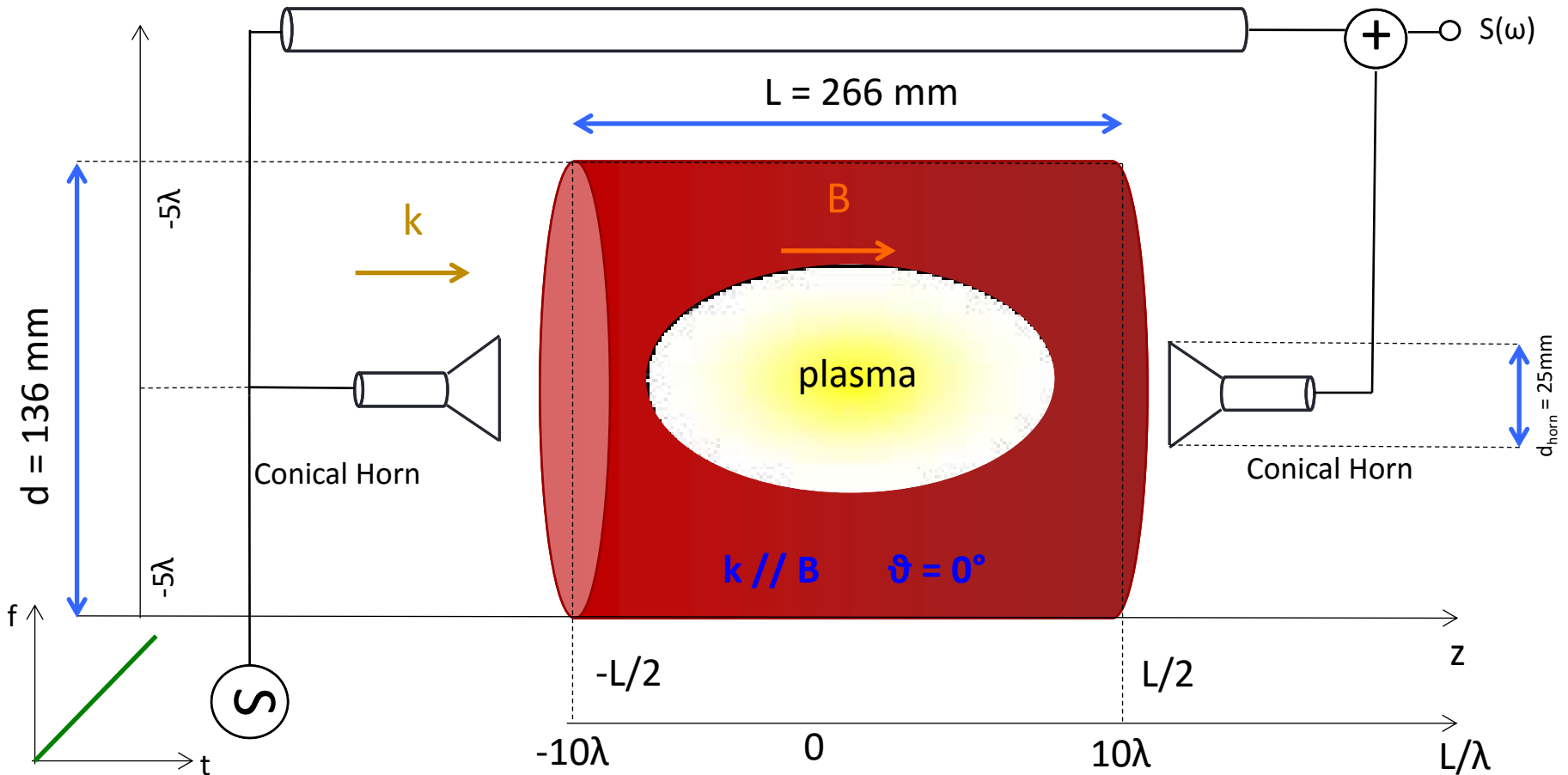
$$\Delta\varphi = \frac{\omega}{c} \left[1 - \left(1 - \frac{\omega_p^2}{\omega^2} \right)^{\frac{1}{2}} \right] L \quad \longrightarrow \quad \omega_p^2 = \frac{4\pi n e^2}{m \epsilon_0}$$

In plasmas the phase variation depends on the “ natural plasma frequency”

The plasma frequency depends on the density

Microwave interferometry measures plasma density through a measurement of phase shift.

Sketch of a Microwave Interferometer

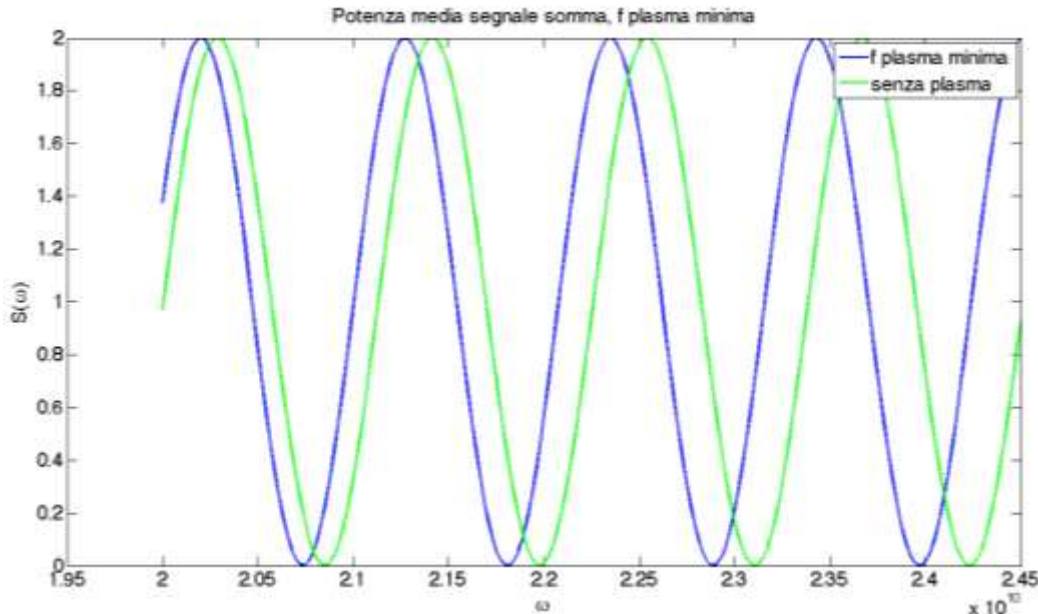


See G. Torrasi et al, Tue PS27

- Limited ECRIS access probing port
- Multi-paths introduce spurious signals

Step 1: Frequency Domain

Parameter	Values
Density min	$n_{e(\min)} = 5 \cdot 10^{17} \text{ e / m}^3$
Density max	$n_{e(\max)} = 4 \cdot 10^{18} \text{ e / m}^3$

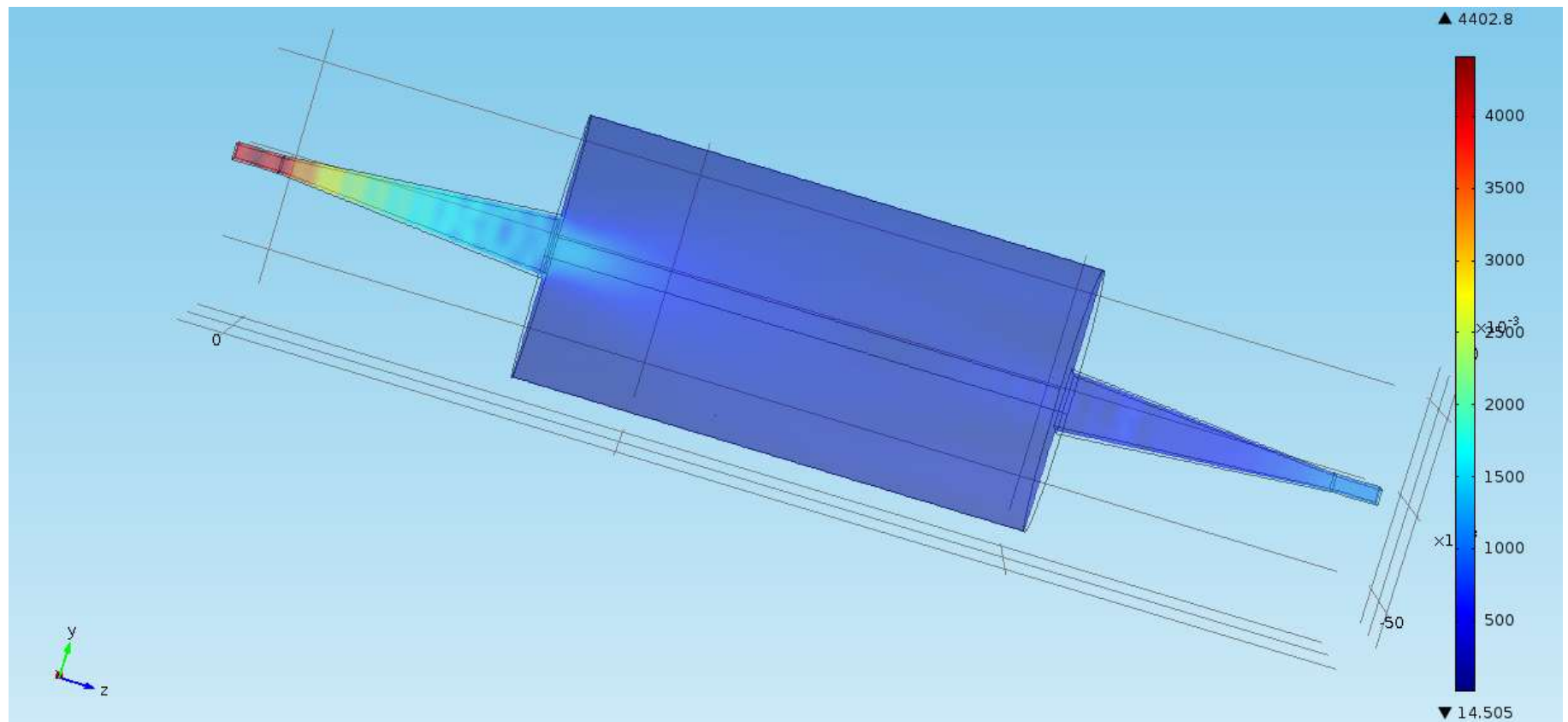


Modification of the beating signal as due to the plasma of minimum density: check of sensitivity

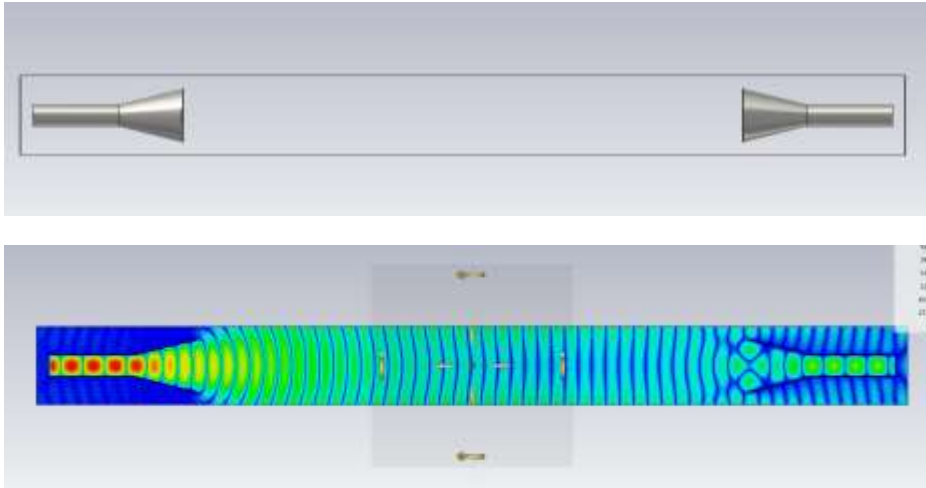
f = 20 – 24.5 GHz

Evaluation done supposing a uniform plasma with uniform permittivity

Specific antenna design avoiding multi-path (spurious) signals detected by the receiving horn



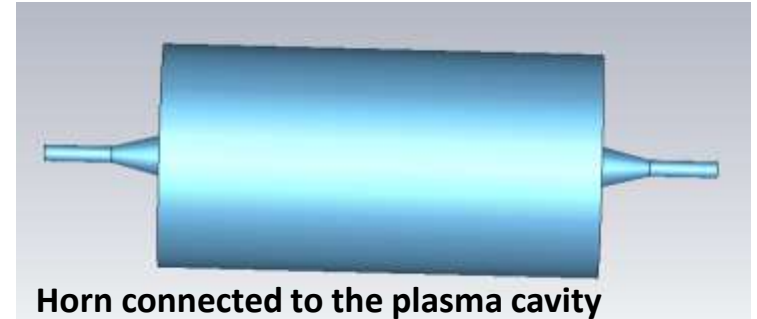
No plasma Horn-to-Horn transmission



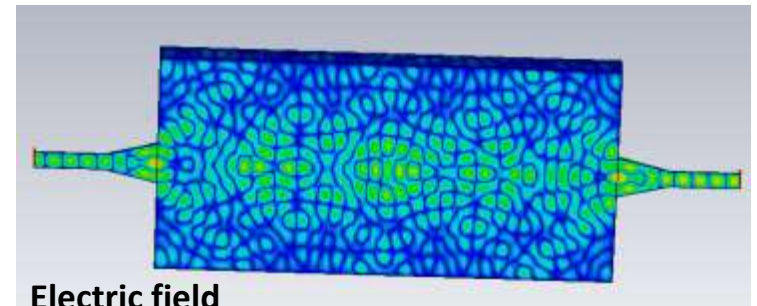
Horn-to-horn transmission for antennas facing each other in vacuum



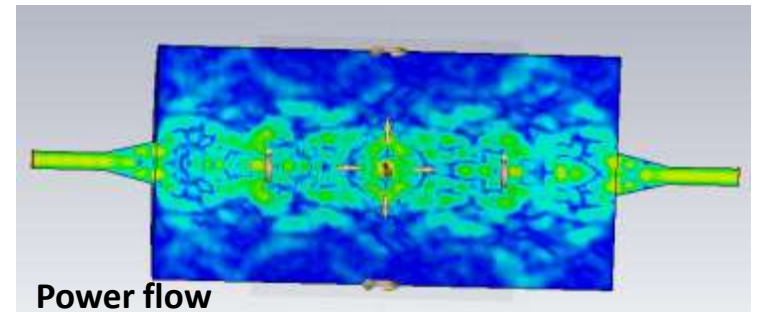
Numerical simulations (COMSOL+CST)
put in evidence cavity walls effects



Horn connected to the plasma cavity



Electric field

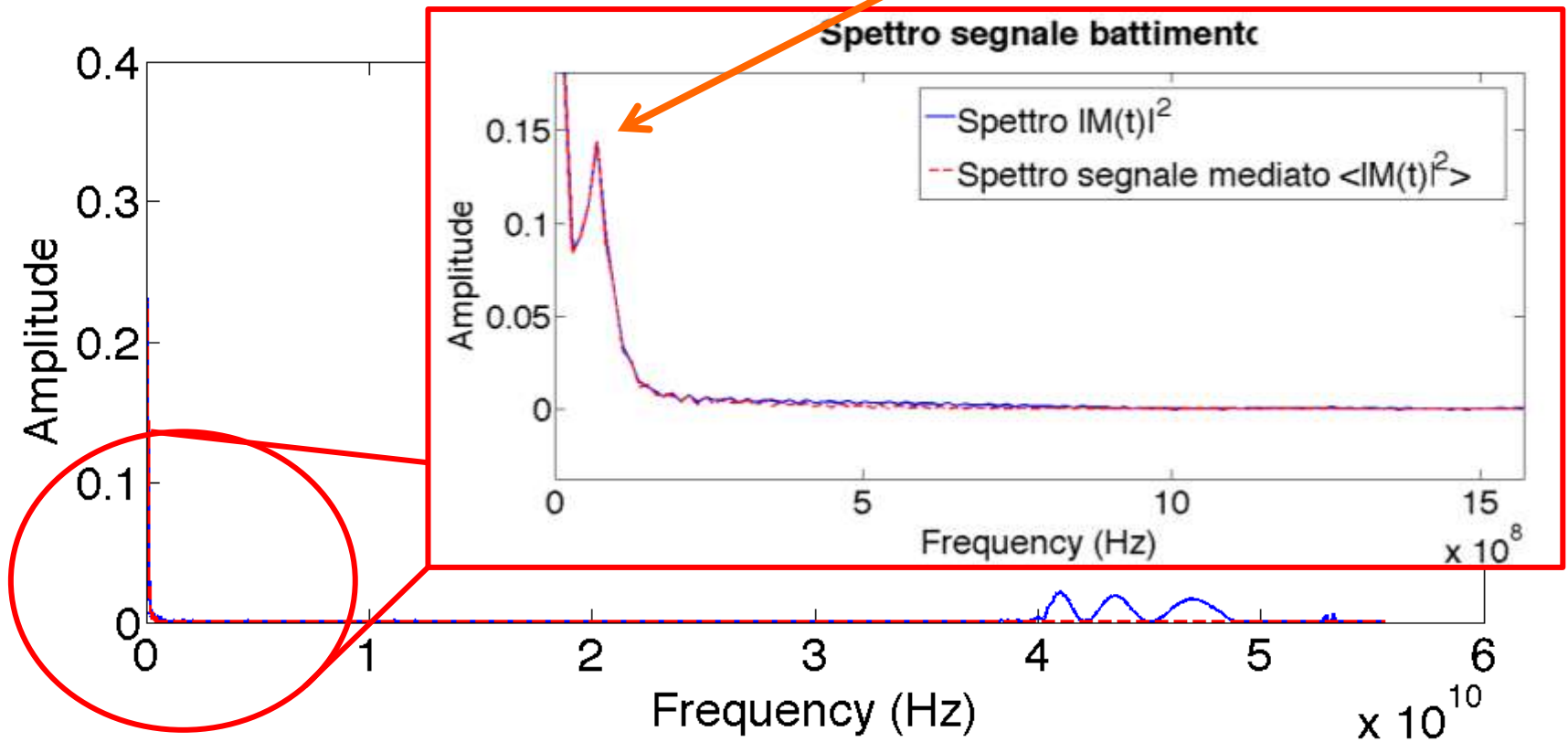


Power flow

Beating signal spectrum (free space)

Reference signal: Waveguide
Probing signal: free space

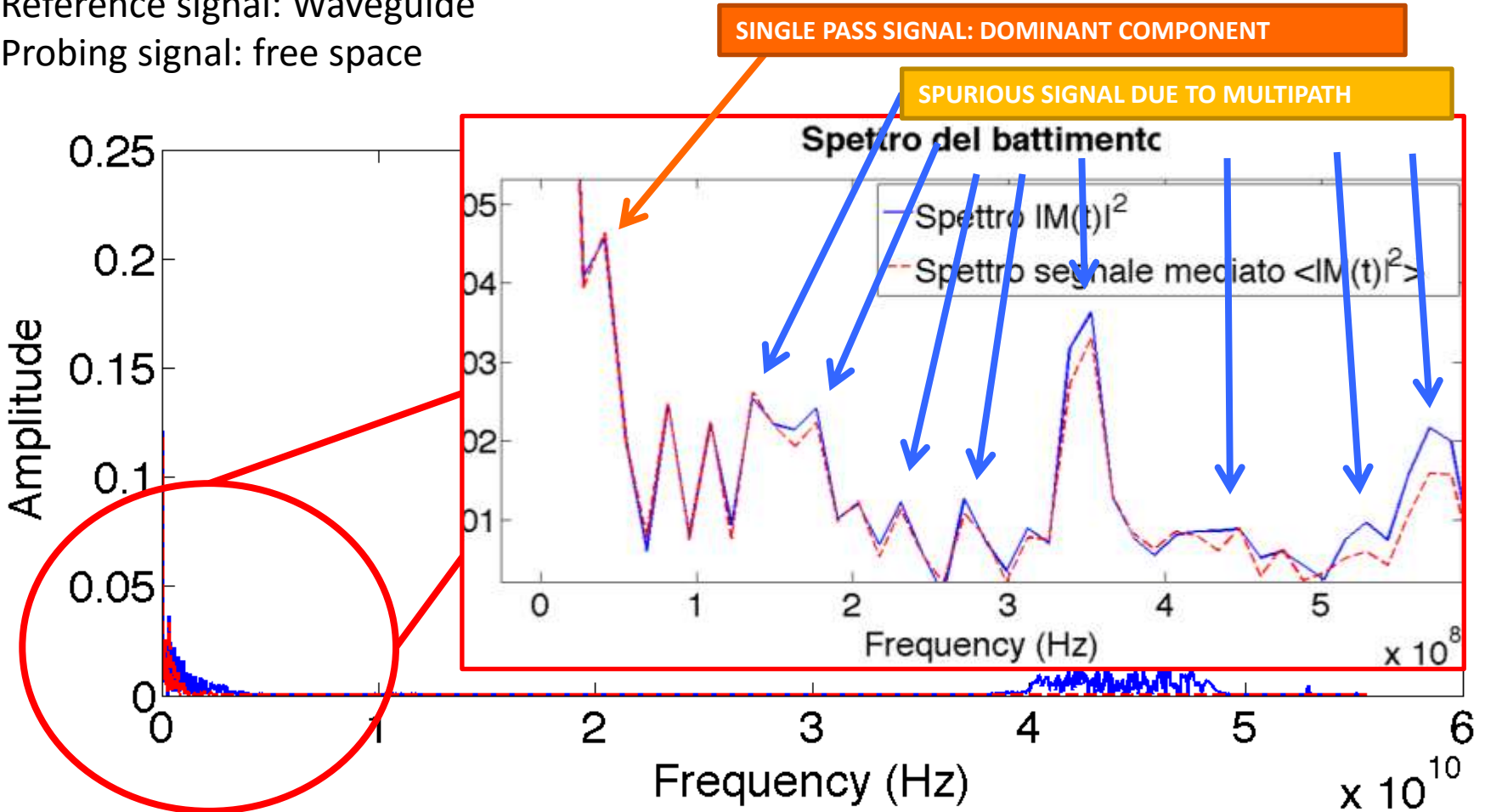
Beating signal component



SIMULATION

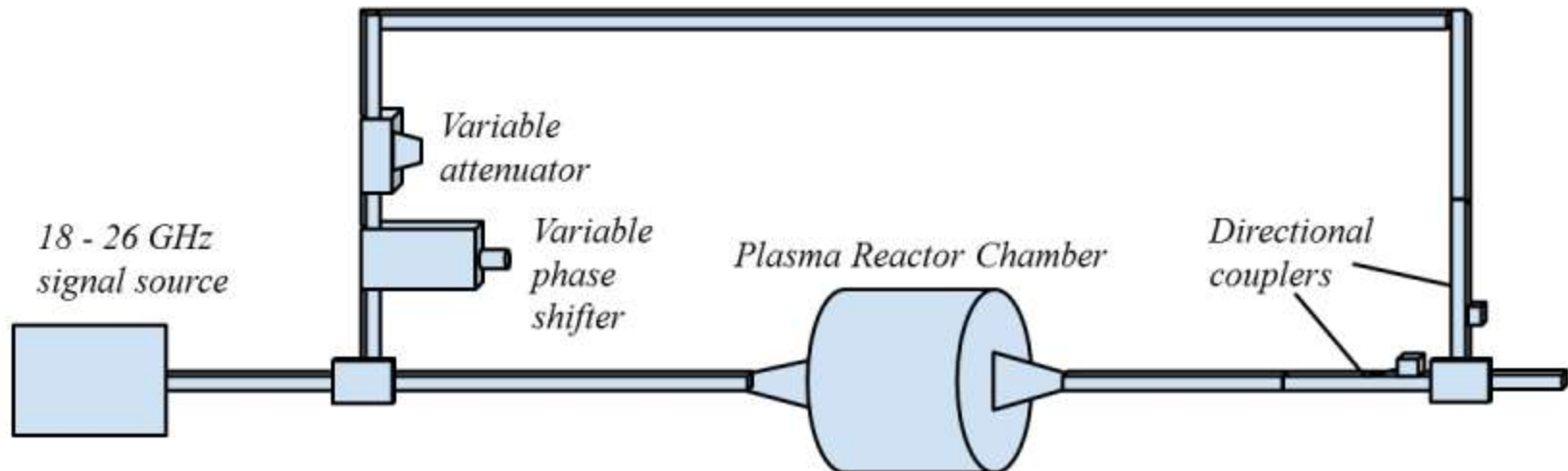
Spectrum of the beating signal when including the cavity

Reference signal: Waveguide
Probing signal: free space



SIMULATION

Implementation



Time averaged Power of the beating signal

$$S(\omega) = 2A^2 \cos^2 \left[\frac{1}{2} \left(\int_L k_{\text{plasma}} dl \right) \right]$$

$$k_{\text{plasma}} = \frac{1}{2} \frac{\omega}{c} \left[\left(\sqrt{1 - \frac{X}{1-Y}} \right) + \left(\sqrt{1 - \frac{X}{1+Y}} \right) \right]$$

Components

See G. Torrasi et al, Tue PS27

Signal Generators

- Anritsu Signal generator
 - YIG oscillator

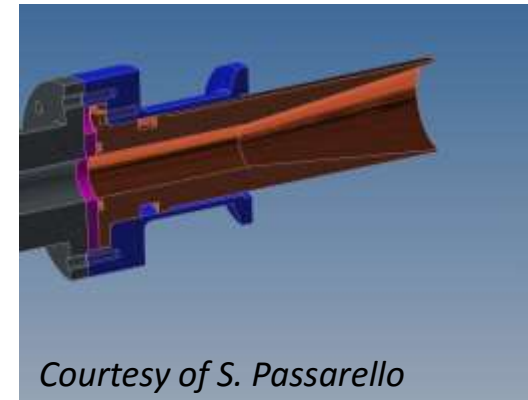


Microwave components



- Phase shifter
- Directional coupler
- Combiner
- E/H-bend, Straight part
- attenuator

Horn antenna fabrication



Courtesy of S. Passarello

Horn assembly

Dimensions :
2.5 cm diameter (DN 25)
Vacuum:
8 μm layer of Kapton



Horn assembly

Dimensions :
2.5 cm diameter
Vacuum:
8 μm layer of K_α

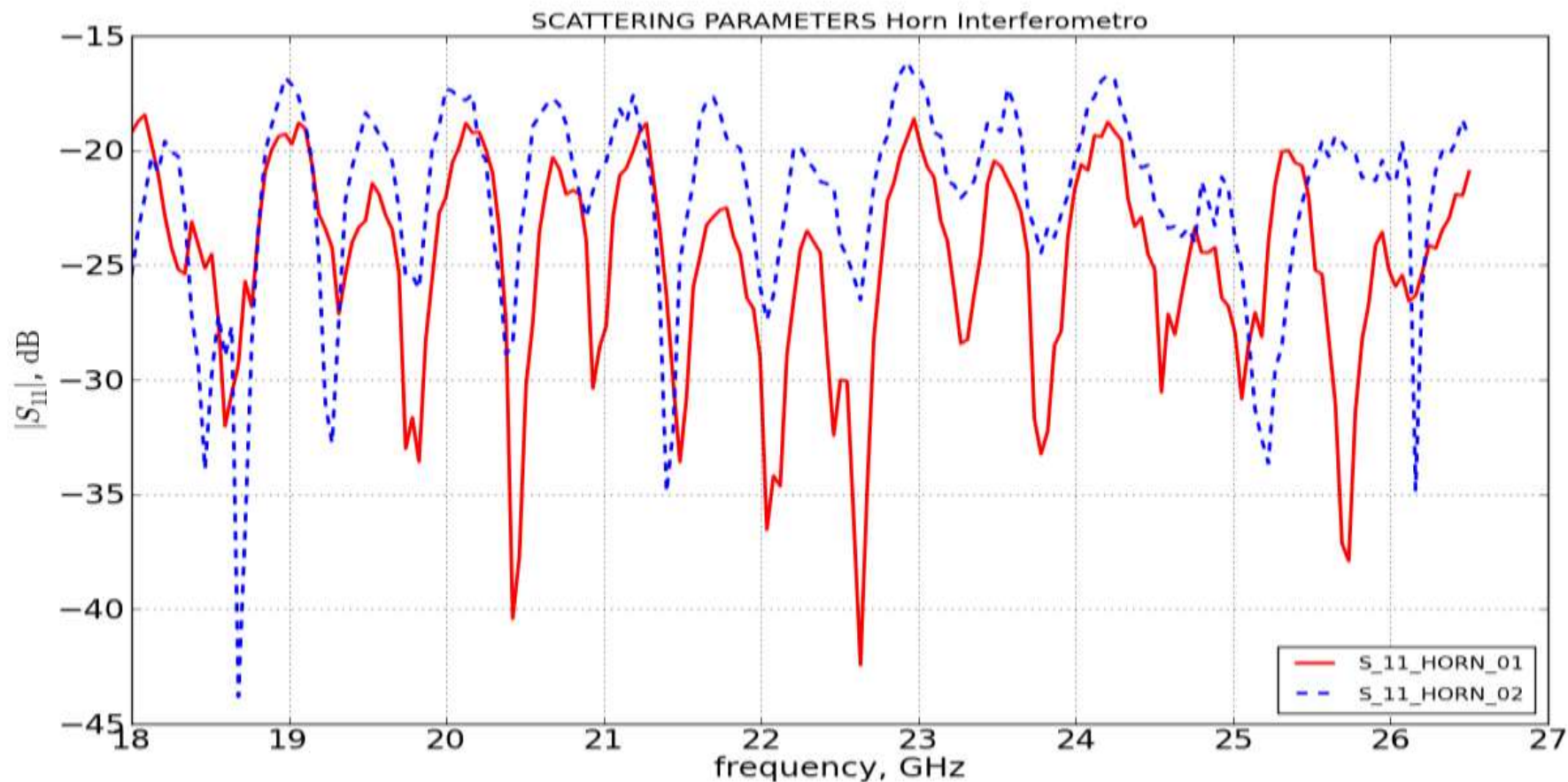
Conical Horn

Optical
diagnostic
windows

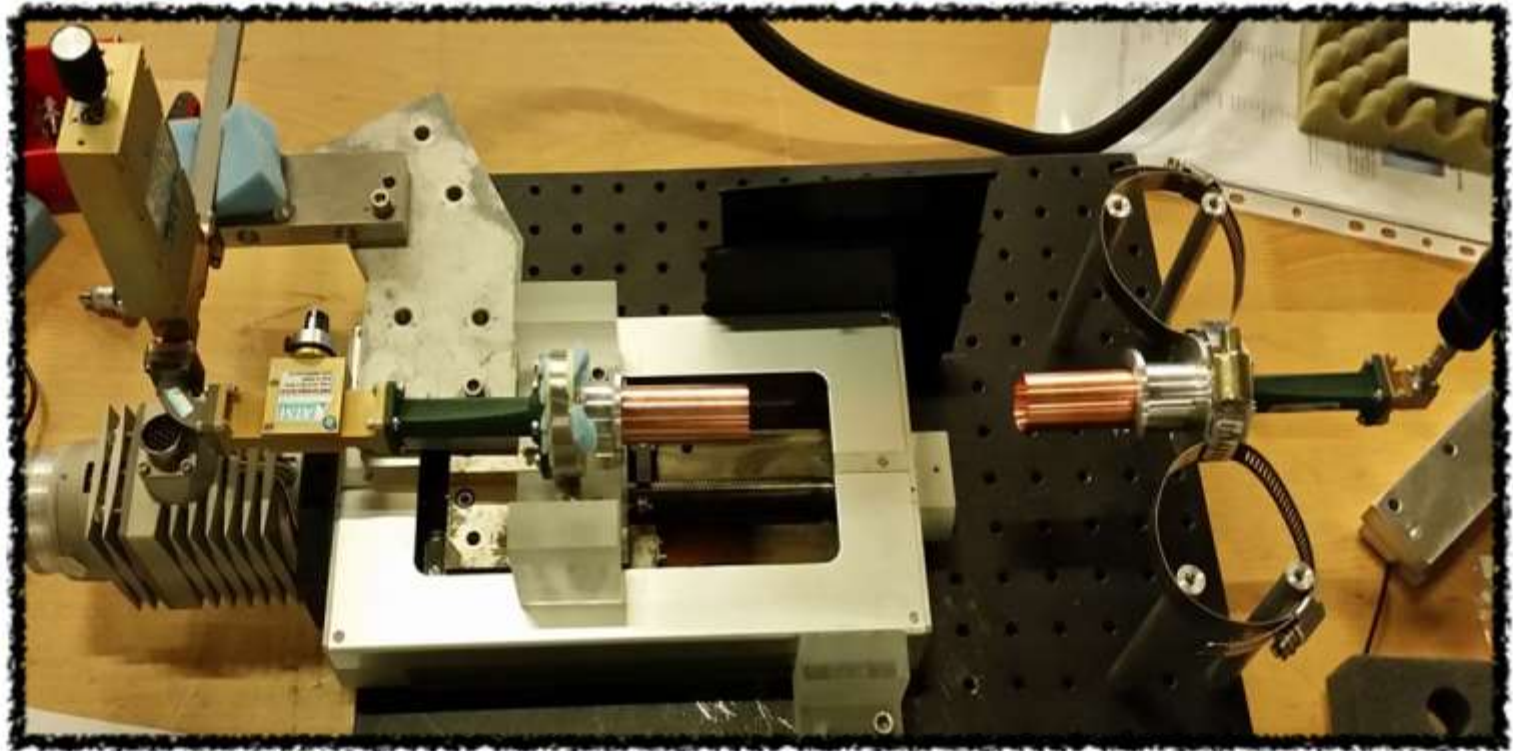
LP flange



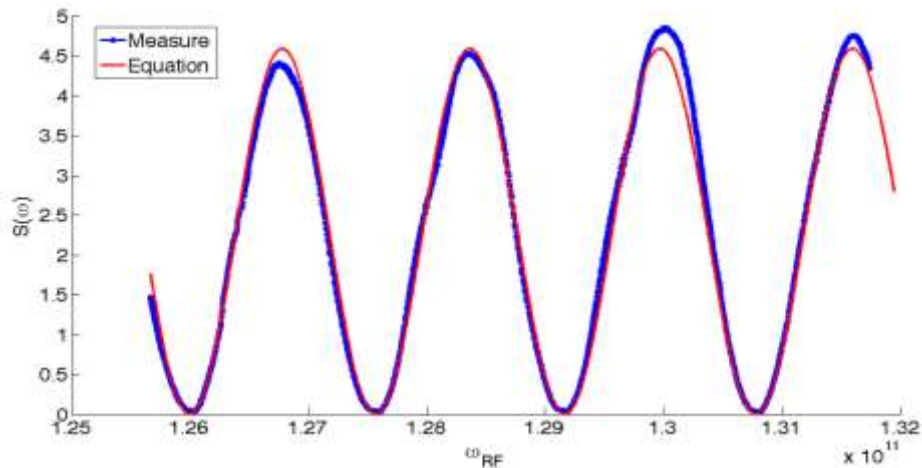
S11 measurement of the horns in the range 18-26.5 GHz



Free space interferometric setup

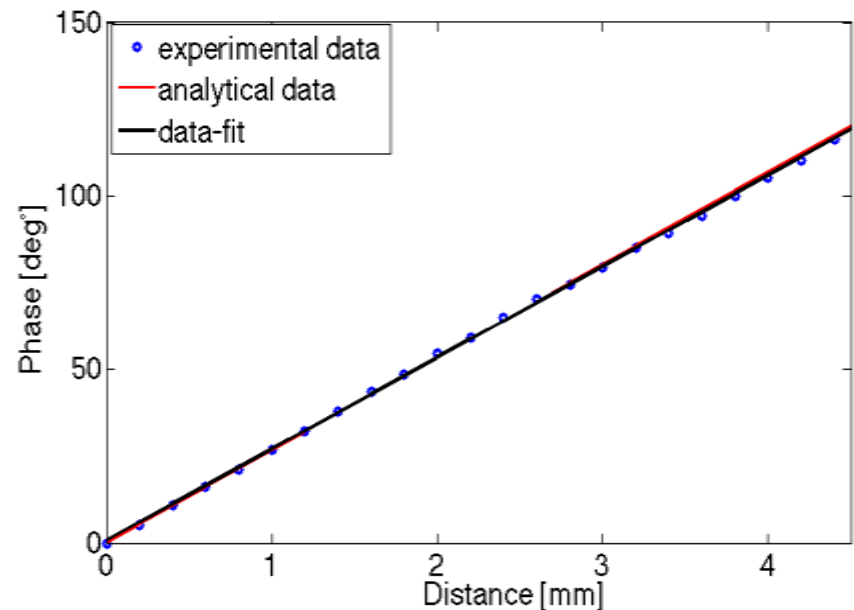


In air beat signal measurement and evaluation of air refractive index

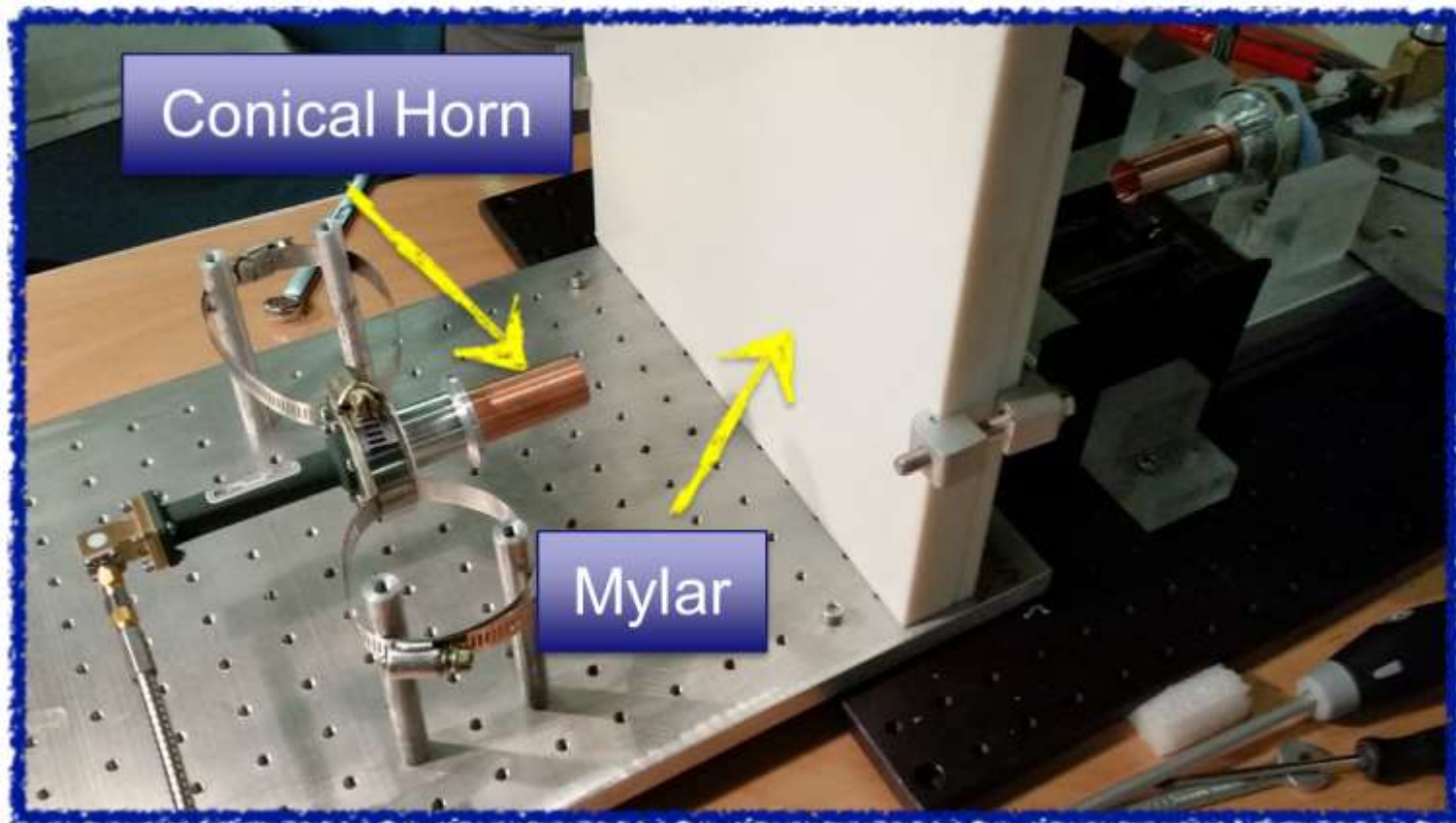


$$S(\omega) \propto 2A^2 \cos^2 \left\{ \left[\Delta L \sqrt{\omega^2 - \omega_c^2} + \omega L \right] / 2c \right\}$$

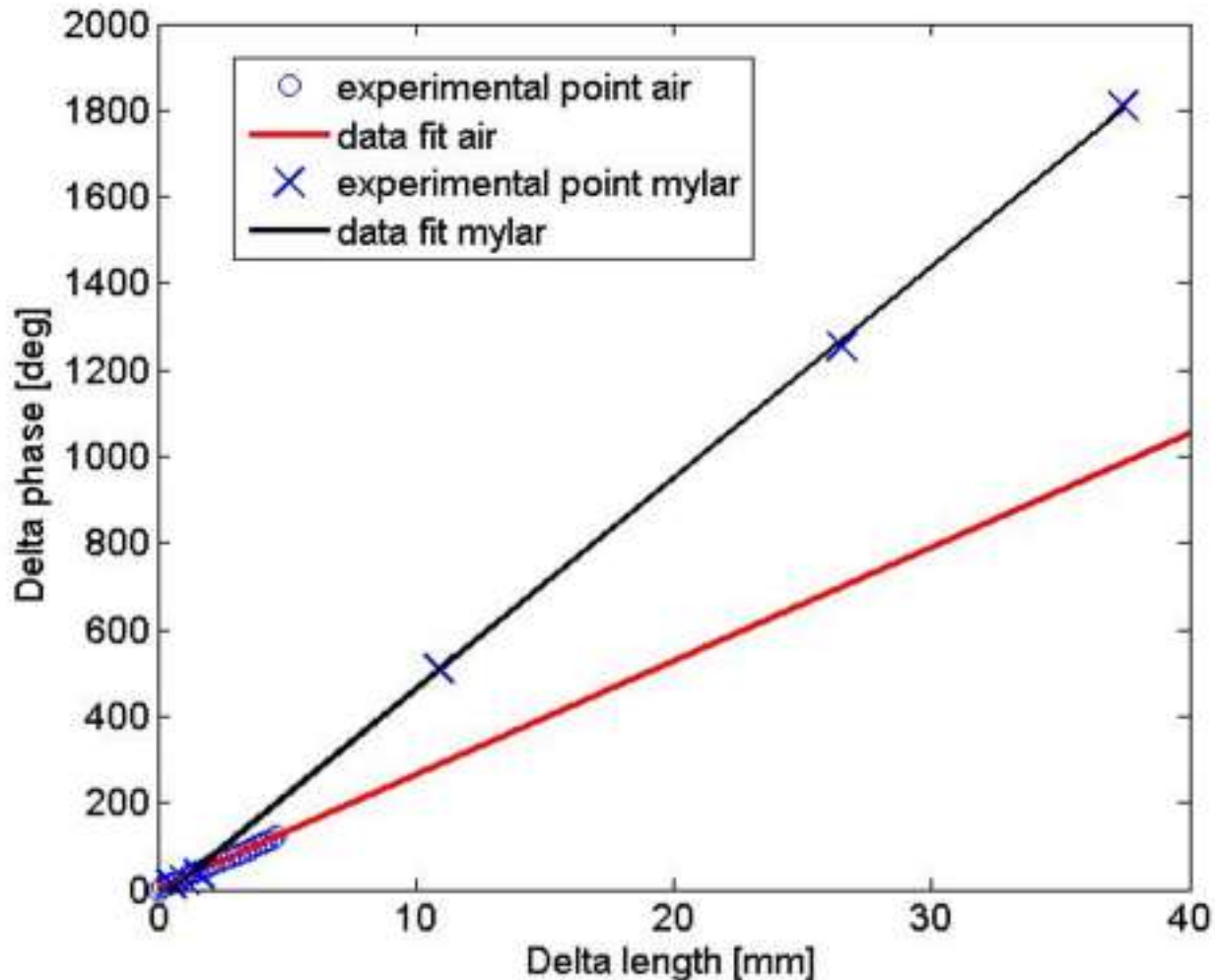
Perfect agreement between
data and calculated value
 $n_{air} = 1$



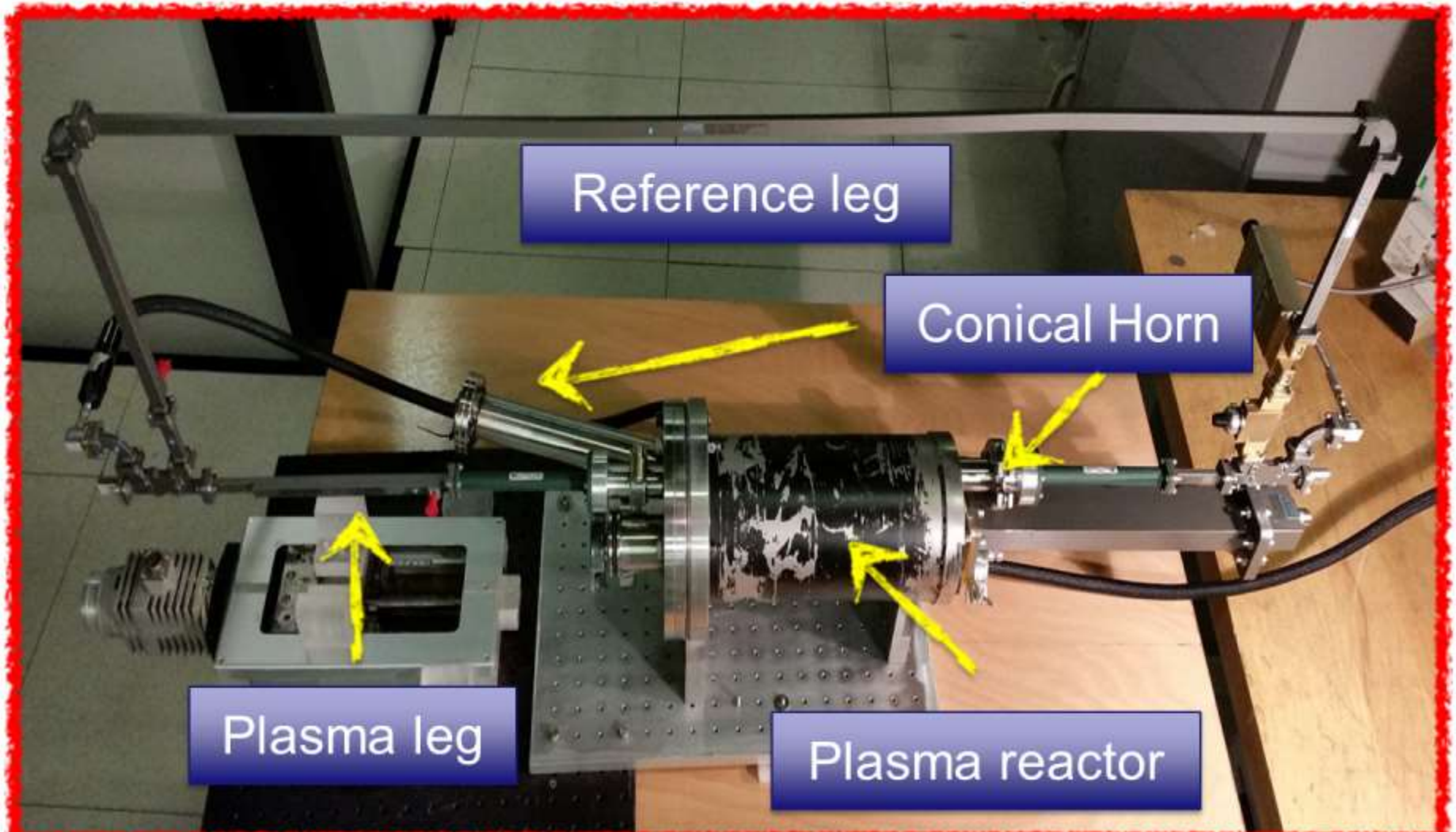
FREE SPACE CHARACTERIZATION : MEASURING THE DIELECTRIC PROPERTIES OF MATERIALS



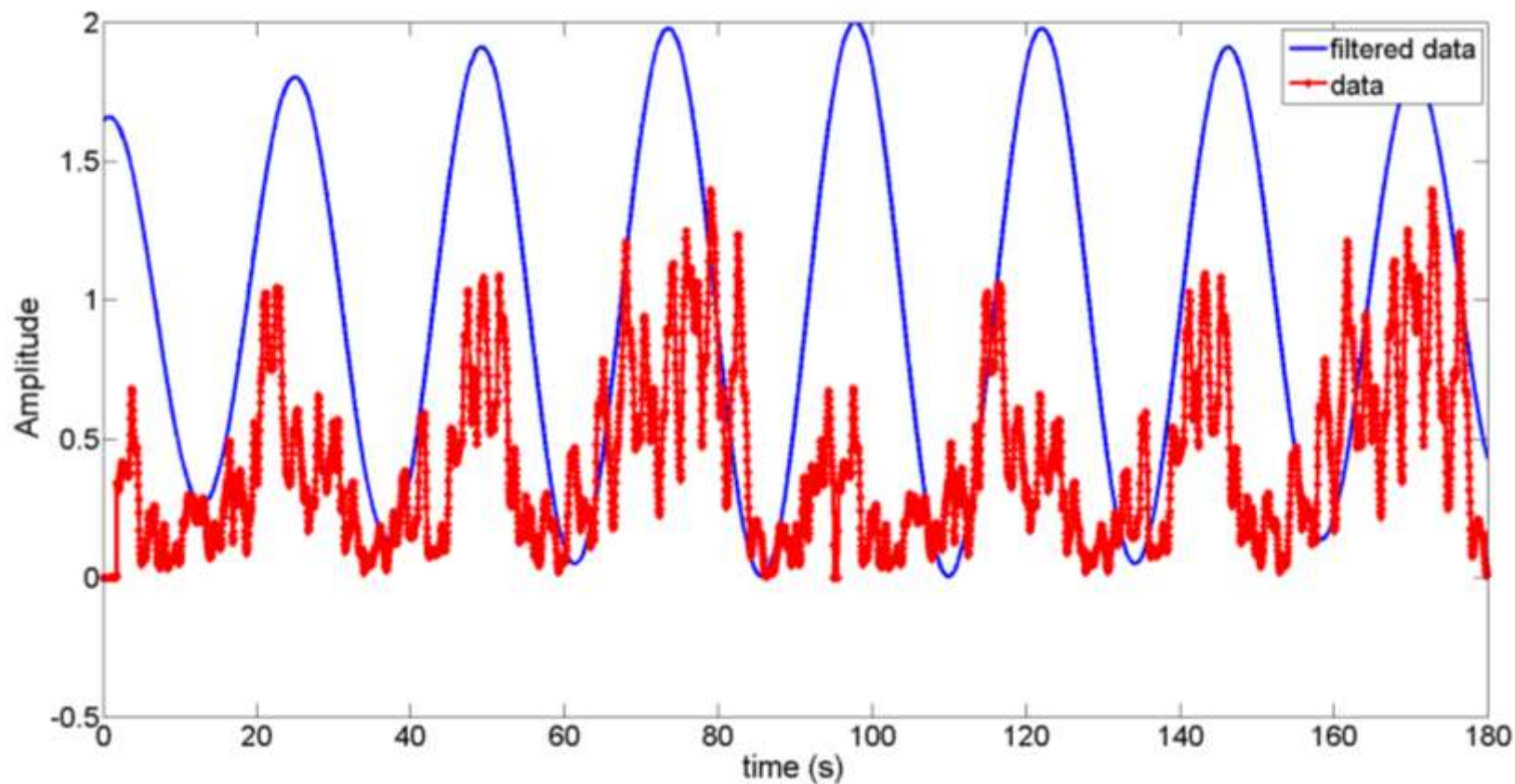
Phase shift as a function of distance between the horn antennas in presence of vacuum and of PETP (Mylar)



Final installation on Plasma Reactor



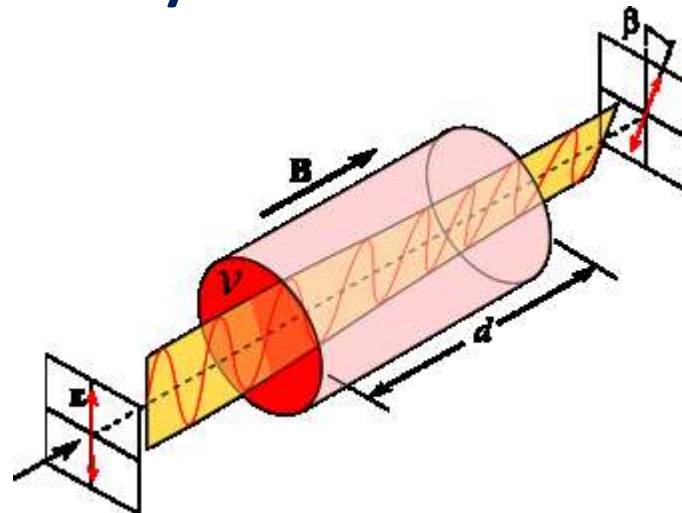
IN CAVITY INTERFEROMETRIC MEASUREMENT



Free space refractive index in cavity reconstructed

Next steps

- Tests with **uniform paraffin cylinder** in progress: noise and multi-path slightly higher with respect to vacuum operations. Strategy to on-line data filtering in progress.
- Tests with **plasma**.
- **Polarimetry (Faraday rotation detection)**

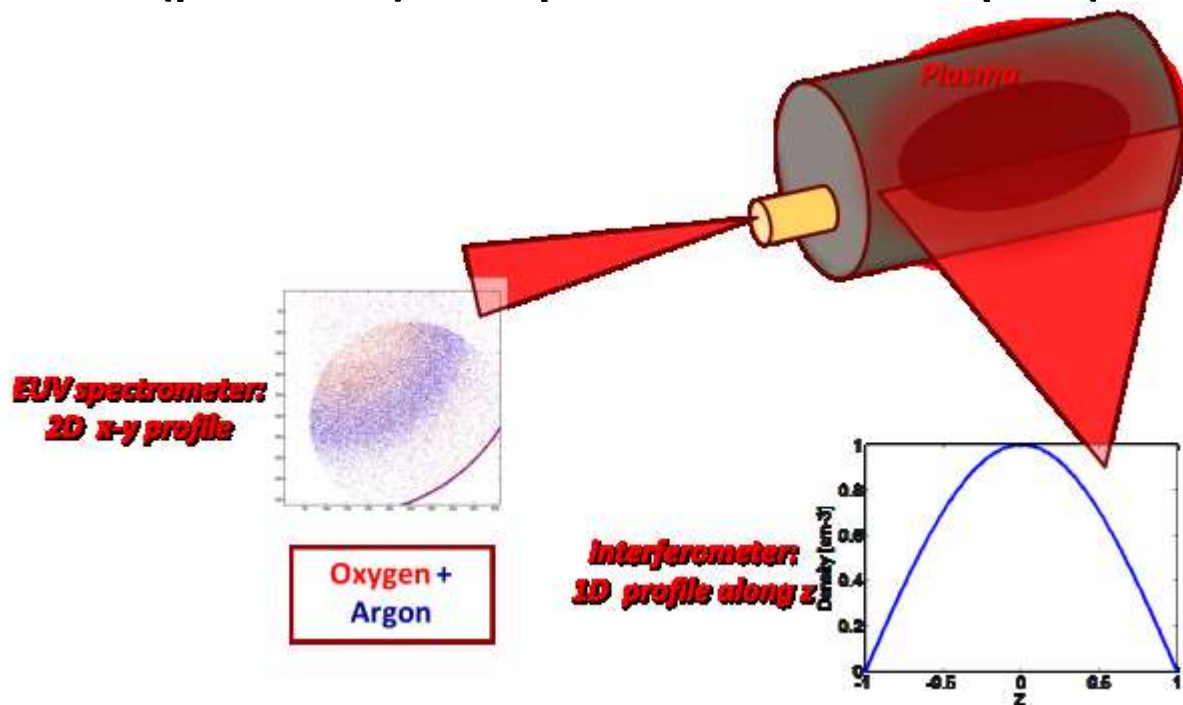


Pros and cons

- Possibility to have a 1D measurement of plasma density.
- The use of multi- horn devices would permit to have a map of density along some reference lines
- **Difficulty of multi probe arrangement in the plasma injection and extraction flanges.**
- **Faster analysis time are needed.**

Perspectives

- Development of a technique to achieve 3D plasma image combining interferometer (profile 1D) and spectrometer techniques (image 2D)



- Development of a new high resolution X-ray spectrometer by means the use of crystal and gratings for ion temperature measurement of on-line evaluation of ion charge state distribution

Conclusions

- Diagnostics developments in synergy with computer simulation and data analysis are the driving force to investigate the phenomena taking place in the ECRIS plasma chamber.
- Fine tuning of frequency and magnetic field permits to optimize current, charge states and beam emittance produced with particular attention to avoid hollow beam production
- Radically different heating mechanism has been successfully tested in a demonstrator and are going to be implemented in the Flexible plasma Trap

Acknowledgments

- **L. Neri,**
- **G. Castro**
- **G. Torrasi**
- **D. Nicolosi**
- **O. Leonardi**